การคายซับสารอินทรีย์ระเหยง่ายบนวัสดุไททาเนต
THE DESORPTION OF VOLATILE ORGANIC COMPOUNDS ON TITANATE BASED MATERIALS

นารายาณ์ เพ็ชรสว่าง
ภัทราพร แก้วมณี
ภัทราพร วิเศษศรี

โครงงานพิเศษนี้เป็นส่วนหนึ่งของการศึกษาตามหลักสูตร
ปริญญาวิทยาศาสตรบัณฑิต (เคมีอุตสาหกรรม)
ภาควิชาเคมี คณะวิทยาศาสตร์
สถาบันเทคโนโลยีพระจอมเกล้าเจ้าคุณทหารลาดกระบัง
ปีการศึกษา 2558

THE DESORPTION OF VOLATILE ORGANIC COMPOUNDS ON TITANATE BASED MATERIALS

NARAYA PECHSAWANG
PATTARAPORN KEAWMANEE
PATTARAPORN VISEDSRI

A SPECIAL PROJECT SUBMITTED IN PARTIAL FULFILLMENT OF
THE REQUIREMENT FOR
THE DEGREE OF BACHELOR OF SCIENCE (INDUSTRIAL CHEMISTRY)
DEPARTMENT OF CHEMISTRY, FACULTY OF SCIENCE
KING MONGKUT'S INSTITUTE OF TECHNOLOGY LADKRABANG
ACADAMIC YEAR 2015

Title	The desorption of volatile organic compounds on titanate based materials
Students	Miss Naraya Pechsawang 55050636
	Miss Pattaraporn Kaewmanee 55050761
	Miss Pattaraporn Visedsri 55050762
Degree	Bachelor of science (Industrial Chemistry)
Academic Year	2015
Advisor	Assoc. Prof. Dr. Tawan Sooknoi
Co-advisor	Dr. Tosapol Maluangnont

Faculty of Science, King Mongkut's Insitute of Technology Ladkrabang (KMITL), has approved this special project submitted in partial fulfillment of the requirement for the degrees of Bachelor of Science (Industrial Chemistry) in academic year 2015.

Committees	Signatures
Asst. Prof. Dr. Sutha Sutthiruangwong Chairperson	
Asst. Prof. Krongkaew Tippayasak Committee	K. Tippayasak
Assoc. Prof. Dr. Tawan Sooknoi Committee and Advisor	
Dr. Tosapol Maluangnont Committee and Co-advisor	T. Maluangnont

Title	The desorption of volatile organic compounds on titanate based materials			
Students	Miss Naraya	Pechsawang	Student ID	55050636
	Miss Pattaraporn	Keawmanee	Student ID	55050761
	Miss Pattaraporn	Visedsri	Student ID	55050762
Degree	Bachelor of science (Industrial Chemistry)			
Department	Chemistry, Faculty of Science KMITL			
Academic Year	2015			
Advisor	Assoc. Prof. Dr. Tawan Sooknoi			
Co-advisor	Dr. Tosapol Maluangnont			

Abstract

This study reports the desorption of some volatile organic compounds (VOCs) namely acetone and acetonitrile on several types of the titanate-based materials. The materials studied include lepidocrocite titanate KZn, K-rKZn and Ba-rKZn, Na-TNW, Na-TNT and Ba-TNT, and commercial P25 TiO_2. The effect of the type of adsorbents for acetone and acetonitrile were investigated employing temperature-programmed desorption (TPD). The titanate nanosheets were prepared via a series of reaction consisting of solid state reaction, proton exchange, exfoliation, followed by the reassembling with KCl or $BaCl_2$. Na-TNW was synthesized by a hydrothermal method, followed by washing or ion exchange when required. Similarly, Na-TNT was obtained from members of this laboratory. The synthesized adsorbents were characterized by powder X-ray diffraction (PXRD) and thermogravimetric analysis (TGA). It is found that lepidocrocite titanate KZn and the K-rKZn and Ba-rKZn do not adsorb both acetone and acetonitrile. The desorption capacity of Na-TNW is lower than that of Na-TNT, Ba-TNT and commercial P25 TiO_2. Ba-TNT shows the highest desorption capacity for both acetone and acetonitrile. This result can be explained considering the high surface area of the nanotube. The amount of acetonitrile desorbed is higher than that of acetone in all cases. It is proposed that the CN group in acetonitrile is more polar than the carbonyl group of acetone. Hence, the interactions between acetonitrile and the nanomaterial absorbent are stronger than those between acetone and the adsorbents.

Keywords: desorption, alkali titanate, nanostructured materials, volatile organic compounds

หัวข้อโครงงานพิเศษ	การคายซับสารอินทรีย์ระเหยง่ายบนวัสดุไททาเนต			
ชื่อนักศึกษา	นางสาว นารายาณ์	เพ็ชรสว่าง	รหัสนักศึกษา	55050636
	นางสาว ภัทราพร	แก้วมณี	รหัสนักศึกษา	55050761
	นางสาว ภัทราพร	วิเศษศรี	รหัสนักศึกษา	55050762
ปริญญา	วิทยาศาสตรบัณฑิต (เคมีอุตสาหกรรม)			
ภาควิชา	เคมี			
คณะ	วิทยาศาสตร์			
มหาวิทยาลัย	สถาบันเทคโนโลยีพระจอมเกล้าเจ้าคุณทหารลาดกระบัง (สจล.)			
ปีการศึกษา	2558			
อาจารย์ที่ปรึกษา	รศ.ดร.ตะวัน สุขน้อย			
อาจารย์ที่ปรึกษาร่วม	ดร.ทศพล เมลืองนนท์			

บทคัดย่อ

โครงงานพิเศษนี้ศึกษาการคายซับสารอินทรีย์ระเหยง่ายคืออะซิโตนและอาซิโตไนไตรล์บนวัสดุไททา-เนตหลายชนิด ได้แก่ เลพิโดโครไซต์ไททาเนต (KZn), เลพิโดโครไซต์ไททาเนตที่ถูกทำให้รวมตัวกันใหม่ด้วยโพแทสเซียมคลอไรด์และแบเรียมคลอไรด์ (K-rKZn และ Ba-rKZn), โซเดียมไททาเนตนาโนไวร์ (Na-TNW), โซเดียม/แบเรียมไททาเนตนาโนทิวบ์ (Na-TNT และ Ba-TNT) และ P25 ไททาเนียมไดออกไซด์ทางการค้า อิทธิพลของวัสดุไททาเนตที่ต่างชนิดกันในการดูดซับอะซิโตนและอาซิโตไนไตรล์ ได้รับการศึกษาโดยเทคนิคการโปรแกรมอุณหภูมิคายซับ (Temperature program desorption) ไททาเนตนาโนชีทจะถูกสังเคราะห์ด้วยชุดปฏิกิริยาต่างๆ คือ ปฏิกิริยาของแข็ง (Solid state synthesis) การแลกเปลี่ยนไอออน (Ion exchange) การแยกออกจากกัน (Exfoliation) และการรวมตัวกันใหม่ด้วยโพแทสเซียมคลอไรด์และแบเรียมคลอไรด์ (Reassembling) ได้สังเคราะห์โซเดียมไททาเนตนาโนไวร์ Na-TNW โดยวิธีไฮโดรเทอร์มอล (Hydrothermal synthesis) และได้รับไททาเนตนาโนทิวบ์จากสมาชิกในห้องแลป ทำการพิสูจน์เอกลักษณ์ของวัสดุดูดซับด้วยวิธีเทคนิคการเลี้ยวเบนของรังสีเอกซ์ (PXRD) และ เทคนิควิเคราะห์ความเสถียรของวัสดุเชิงความร้อน (TGA) พบว่า KZn, K-rKZn และ Ba-rKZn ไม่เกิดการคายซับทั้งของอะซิโตนและอาซิโตไน-ไตรล์ การคายซับของอะซิโตนและอาซิโตไนไตรล์ใน Na-TNW น้อยกว่า Na-TNT Ba-TNT และ P25 ไททาเนียมไดออกไซด์ทางการค้า Ba-TNT ให้ค่าการคายซับมากที่สุดทั้งอะซิโตนและอาซิโตไนไตรล์ ผลการทดสอบเหล่านี้สามารถอธิบายได้จากพื้นที่ผิวที่มากของไททาเนตนาโนทิวบ์ การคายซับอาซิโตไนไตรล์มากกว่าการคายซับอะซิโตนในทุกกรณี อาจอธิบายได้ว่าอาซิโตไนไตรล์มีหมู่ฟังก์ชันจำพวกไซยาไนด์ซึ่งมีความเป็นขั้วมากกว่าหมู่ฟังก์ชันจำพวกคาร์บอนิลของอะซิโตน ดังนั้นอันตรกิริยาระหว่างอาซิโตไนไตรล์กับวัสดุดูดซับนาโนจึงมีความแข็งแรงกว่าอันตรกิริยาระหว่างอะซิโตนกับวัสดุดูดซับ

คำสำคัญ : การคายซับ, แอลคาไลไททาเนต, วัสดุที่มีโครงสร้างระดับนาโน, สารอินทรีย์ระเหยง่าย

ACKNOWLEDGEMENTS

The authors would like to acknowledge the project advisor and co-advisor, Assoc. Prof. Dr. Tawan Sooknoi and Dr. Tosapol Maluangnont respectively, for their support, supervision, inspiration, suggestion and encouragement throughout our this work.

We are also greatly thankful for Asst. Prof. Dr. Sutha Sutthiruangwong and Asst. Prof. Krongkaew Tippayasak who serve as the chairperson and the committee.

We are also greatly appreciated the financial support from the Department of Chemistry, Faculty of Science, King Mongkut's Institute of Technology Ladkrabang. We would like to specifically thank Mr. Boonyawat Wuttitham for his help and advice in experimental parts and the data analysis. We thank Laphatrada Boonsiriwikorn, Waminee Niramit and Wiranya Chansataporn for providing us the Na-TNT and Ba-TNT, including the specific surface area data. We would also like to thank the member of the catalytic chemistry research unit (CCR).

Finally, we thank our families for their supports.

Naraya Pechsawang
Pattaraporn Keawmanee
Pattaraporn Visedsri

ABBREVIATIONS

Lepidocrocite titanate KZn	=	Lepidocrocite titanate $K_{0.8}Zn_{0.4}Ti_{1.6}O_4$
K-rKZn	=	Lepidocrocite titanate $K_{0.8}Zn_{0.4}Ti_{1.6}O_4$ reassembled with KCl
Ba-rKZn	=	Lepidocrocite titanate $K_{0.8}Zn_{0.4}Ti_{1.6}O_4$ reassembled with $BaCl_2$
Na-TNW	=	Sodium titanate nanowire
Na-TNT	=	Sodium titanate nanotube
Ba-TNT	=	Barium titanate nanotube

CONTENTS

CONTENTS (continued)

LIST OF TABLES

LIST OF SCHEMES

LIST OF FIGURES

LIST OF FIGURES (continued)

CHAPTER1

INTRODUCTION

1.1 Motivation

Volatile Organic Compounds (VOCs) are harmful compounds which can be found both outdoor and indoor. They are organic compounds with low boiling point and are easily volatile at room temperature. Examples of VOCs include aromatics such as benzene, hydrocarbons such as hexane, chlorinated compounds such as trichloroethane, or oxygen-containing compounds such as acetone. The chemical structure of acetone and acetonitrile which is of interest in this project is shown in **Figure 1a** and **b** respectively. So, there is a need to develop materials which can absorb VOCs such that these harmful materials are removed from the environment in a later step.

(a) (b)

Figure 1 Chemical structure of (a) acetone, (b) acetonitrile.

Titanium dioxide (TiO_2) have found wide use in various applications such as cosmetic, self-cleaning surface, air system coating, paint and etc. because it is cheap, chemically stable, and nontoxic. In recent years, there are reports on the use of commercial TiO_2 to adsorb and photochemically decompose VOC [1]. The important physical property for such application is a high surface area of the material. However, the influence of the crystal structure on the adsorption has received little attention. It is not clear how VOCs desorb from these materials. In addition to TiO_2, there are several solids with related crystal structure known as alkali titanates comprising of alkali metal cations, titanium, and oxygens. The study of these solids as sorbents (in addition to the well-known ones of TiO_2 such as anatase, rutile, brookite) might provide more understanding on the mechanism of VOC adsorption/desorption.

Also, typical materials crystallize into objects in the micrometer-range (or larger), resulting in relatively small surface. The small surface area then limits the adsorption of gaseous molecules. One solution to solve this problem is to use nanomaterials as adsorbents. The titanate can exist in several nanostructures, such as (bulk) microcrystal, nanotubes, nanowires, etc. These nanostructures are in fact constructed from the stacks of layers having the charge balancing cations in between. Besides, in some structure the layers can be separated by a process called exfoliation, and further reconstructed to give a higher-surface area material [2-3].

In this work, we will study the use of microcrystals of alkali titanate of several compositions with related structure such as lepidocrocite titanate KZn, the K-rKZn and Ba-rKZn made from lepidocrocite titanate KZn, Na-TNW, Na-TNT and Ba-TNT. We will also prepare Na-TNW. These titanate-based materials will be used as the sorbent for model compounds **(Figure 1)** representing various types of VOCs.

1.2 Objectives

1.2.1 To obtain the different titanates including lepidocrocite titanate KZn, the K-rKZn and Ba-rKZn made from lepidocrocite titanate KZn, sodium trititanate ($Na_2Ti_3O_7$), Na-TNW, Na-TNT and Ba-TNT.

1.2.2 To study the effect of the titanate nanostructures, crystal structure, and surface area on the desorption of various volatile organic compounds.

1.3 Scopes of study

1.3.1 Synthesis of microcrystalline lepidrococite titanate KZn. The sodium trititanate ($Na_2Ti_3O_7$) can also be synthesized similarly and the synthesis of Na-TNW is from the hydrothermal method.

1.3.2 Exfoliation of protonated lepidocrocite titanate ($H_{1.6}\square_{0.4}Ti_{1.6}O_4\cdot 0.8H_2O$) by tetrabutylammonium hydroxide (TBAOH), and reassembling the colloidal suspension with potassium chloride and barium chloride and protonated trititanate ($H_2Ti_3O_7$) was exfoliated with tetrametylammonium hydroxide (TMAOH).

1.3.3 Characterization of the solids/suspensions by X-ray Diffraction (XRD), thermogravimetric analysis (TGA) and UV-VIS spectroscopy.

1.3.4 Testing on the desorption of acetone and acetonitrile in a fixed bed system.

1.4 Expected results

It is expected that a better understanding of the effect of the nanostructures, crystal structures, and surface area of titanate-based materials on the desorption of VOCs (acetone and acetonitrile) will be obtained.

CHAPTER 2

THEORY AND LITERATURE REVIEWS

2.1 Volatile organic compounds

Volatile organic compounds (VOCs) are organic compounds that easily evaporate into the air at room temperature and normal pressure [4]. The boiling point of common VOCs is less than or equal to 250 $^{\circ}$C at 1 atm [5]. While most of them contain just carbon atoms and hydrogen atoms, some also contains hetero-elements such as oxygen atoms and chlorine atoms.

The exposure to VOCs in everyday life comes from several sources such as paints, pesticides, solvents in printing, and also from workplaces such as laboratories, industrial factories, petroleum refineries, petrochemical plants, pharmaceutical industry, etc. VOCs might be released into the air, water, food and drinks. VOCs that are collected inside the body for a long time will be hazardous to several systems of human [6, 7] such as respiratory system, central nervous system, immune system. Small side effects include headache, sleepiness and dizziness. The level of hazards will be more or less dependent on the type and diversity of chemicals [8]. Some specific chemicals will be described in detail below.

2.1.1 Acetone

Acetone (**Figure 2.1**) is the organic compound with the chemical formula $(CH_3)_2CO$. It is also called propanone in IUPAC nomenclature. It is a volatile, colorless, and flammable liquid with the melting point of -95.4 ° C and the boiling point of 56.53 ° C. Acetone is soluble in water, ethanol and ether [9]. It is used as a solvent in manufacturing processes in industries such as the chemical industry, pharmaceutical manufacturing, paints, inks, adhesives, lacquers, varnish, cosmetics and plastics industry. Moreover, acetone is also widely used in laboratories as a common solvent for rinsing laboratory glassware. In daily life, it is the primary component in cleaning agents such as nail polish remover [9, 10]. Although acetone has many benefits, it is hazardous to several organs [11, 12].

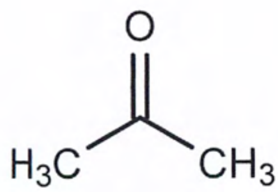

Figure 2.1 The molecular structure of acetone [13].

2.1.2 Acetonitrile

Acetonitrile is organic nitrile compound CH_3CN. It has the cyanide group attached carbon atom. The structure of acetonitrile is shown in the **Figure 2.2** [14]. Acetonitrile is colorless liquid, flammable and poisonous in small dose. It is produced as byproduct from acrylonitrile synthesis. It has sweet and ethereal ardor with melting point at -46 °C and boiling point at 81.6 °C [14, 15]. It is used mainly an organic solvent in the purification of butadiene and in the battery production because of its ability to dissolve electrolytes. In the laboratory, It can be dissolved in range of the ionic and nonpolar compounds and it is used a solvent as a mobile phase in the HPLC Moreover, it is used as a solvent for manufacturing pharmaceuticals and photographic films [14].

Figure 2.2 The molecular structure of acetonitrile [14].

2.2 Titanium dioxide

Titanium dioxide is commonly used in many applications because it is a highly stable, non-toxic, and cheap material. Common crystalline phases of titanium dioxide are divided into three types (**Figure 2.3**) including rutile, anatase and brookite. Rutile has a tetragonal structure, anatase has a tetragonal structure, and brookite has an orthorhombic structure [17]. Titanium dioxide has found widespread uses in several applications such as paintings and cosmetics. Moreover, it is commonly applied to photochemically degrade pollutants such as VOCs [16].

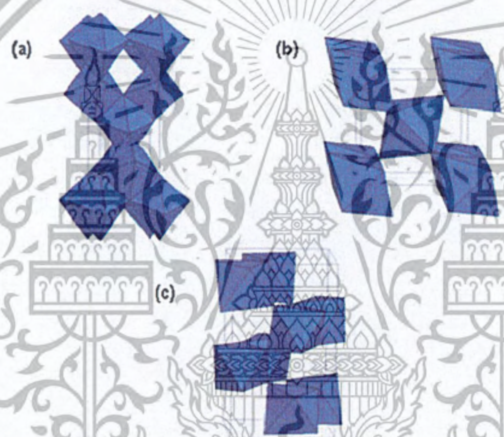

Figure 2.3 The crystal structure of TiO_2: (a) anatase, (b) rutile, and (c) brookite [17].

2.3 Sodium tri-titanate ($Na_2Ti_3O_7$)

The trititanate crystals are build up by the interconnection of three TiO_6 octahedra which share edges. These chains of octahedra join at the corners to form a stepped, zigzag ribbon layered structure [18]. The crystal structure of sodium trititanate ($Na_2Ti_3O_7$) is shown in **Figure 2.4** [19]. In this study we synthesize sodium trititanate ($Na_2Ti_3O_7$) by a solid state method. The structure of sodium trititanate ($Na_2Ti_3O_7$) is different from structure of lepidocrocite obviously.

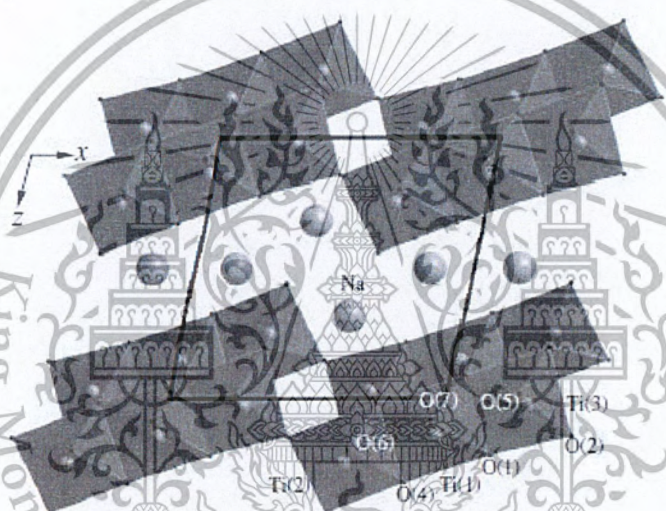

Figure 2.4 The crystal structure of sodium trititanate ($Na_2Ti_3O_7$) [19].

2.4 Lepidocrocite titanate

Lepidocrocite titanate (**Figure 2.5**) is a layered metal oxide with a general formula $H_xTi_{2-x/4}\square_{x/4}O_4$ ($x \sim 0.7$; $\square$ is the vacancy). The lepidocrocite (γ-FeOOH)-type layered structure can be conveniently prepared by a solid-state method. This titanate has excellent ion-exchange reactivity where inorganic and/or organic cations and surfactants can be accommodated. The layers can be ultimately separated into unilamellar sheets by the process called exfoliation. So a large number of extremely thin sheets capable of exhibiting relatively high surface area. In recent years, lepidocrocite titanate has received great attention due to its interesting interlayer chemistry and physical properties [20, 21]. Lepidocrocite titanate has been widely studied as a precursor for the synthesis of nanostructured materials as will be discussed briefly below.

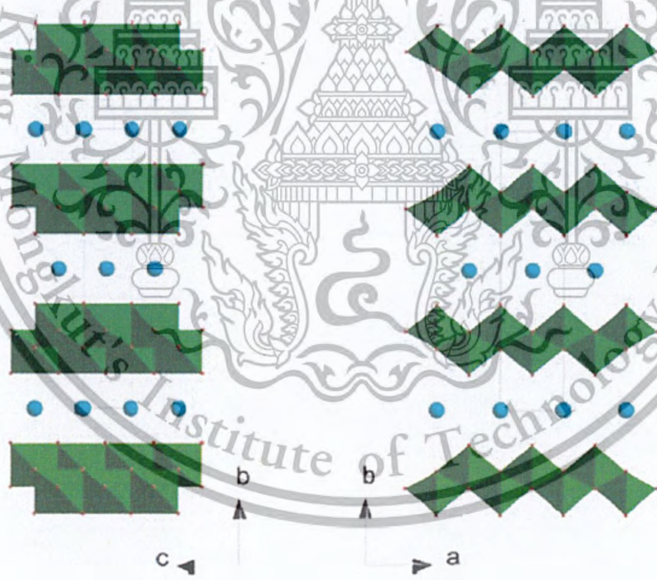

Figure 2.5 The crystal structure of lepidocrocite titanate. The blue dots are the alkali metal cations, while the green objects are the TiO_6 octahedra linked via the edges [20, 21].

2.5 Nanostructures

Nanostructured materials have high surface area, quantum size effects, and significantly enhanced kinetics etc. These properties typically result in superior chemical/physical properties compared to bulk solids. Main types of nanostructured materials are known including zero-dimensional (0D), one-dimensional (1D), two-dimensional (2D) and three-dimensional (3D) nanomaterials as shown in **Figure 2.6**. The zero-dimensional (0D) materials include clusters, quantum dots and nanodots. The one-dimensional (1D) materials include nanotube, nanorod, and nanowire. The two-dimensional (2D) materials include nanosheet, nanofilm, nanolayer, and nanocoating.

Figure 2.6 The classifications of nanostructure materials into 0D, 1D, and 2D [22].

Nanowire (**Figure 2.7**) is a one-dimensional (1D) nanostructure that has an extremely small diameter on the order of a few nanometers (nm) or less, while the length can be up to the micrometer-range. The synthesis of TiO_2 nanowire from P25 TiO_2 by a hydrothermal method has been reported [23]. Several applications of titanate nanowire have been reported including photocatalysis, nanoelectronics and photo-electrochemical applications [24].

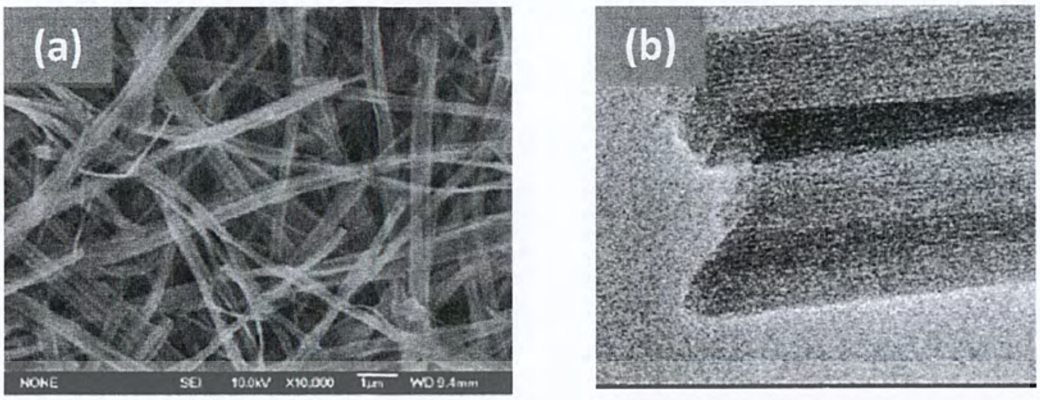

Figure 2.7 SEM images of (a) as-synthesized titanate nanowire (b) high resolution TEM images of as-synthesized titanate nanowire [25].

Nanotube (**Figure 2.8**) is the one-dimensional (1D) nanostructure materials having a tubular structure. The diameter is in the range 8-10 nm while the length can be in the range 50-200 nm. Titanate nanotube has high surface area, excellent photocatalytic activity, and uniform nanometer-size channels. The easiest method of synthesis is the hydrothermal treatment with alkali solution under mild temperature and pressure conditions [26, 27]. It is interesting to study the desorption behavior of these two types of 1D nanostructure, one is relatively dense (nanowire) and the other is more open (nanotube).

Figure 2.8 TEM images of titanate nanotube at (a) low and (b) high magnification [27]. The scale bar is 50 micrometer in (a) and 10 nanometers in (b).

Nanosheet is a two-dimensional (2D) nanostructure which is atomically thin, with the thickness in a range 1 to 100 nm [28]. The sheet is very flexible. With appropriate reassembling, nanosheet could be fabricated into high-surface area materials [29]. Specifically, titanate nanosheet (**Figure 2.9**) can be synthesized via a liquid-phase exfoliation of the layered protonic titanate precursor. The negatively-charged layers are naturally bound to each other by weak van der Waals interactions, and the charge neutrality is accomplished by cations residing at the interlayer space. In liquid-phase exfoliation, these single sheets of layered materials can be separated by using an appropriate solvent, creating the colloidal suspensions of unilamellar sheets. Titanate nanosheets have been found to be very effective as adsorbent and photocatalysts, thanks to their two-dimensional geometry [30].

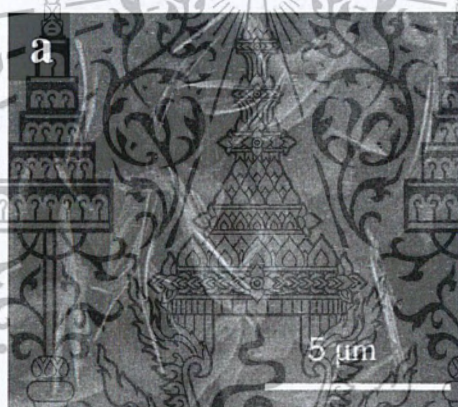

Figure 2.9 (a) Field emission scanning electron microscopy (FESEM) image of as-synthesized anatase TiO_2 nanosheet [31].

2.6 Adsorption/Desorption

Adsorption is the interaction between adsorbate and adsorbent in which atoms, ions or molecules from gas, liquid or solid state are attached to a surface of the adsorbent. The high surface area of sorbent can make a good adsorption capacity [32, 33].

Adsorption can be classified as physisorption and chemisorption. Physisorption is the adsorption where the forces between the molecules of the adsorbate and the adsorbent are of Van der Waal's type. In physical adsorption, the forces of attraction between the adsorbate and adsorbent are very weak. Therefore, the adsorbate/adsorbent interactions can be easily overcome by heating to elevated temperature or by decreasing the pressure. The most suitable conditions for physisorption are low temperature and low pressure. On the other hand, chemisorption is the adsorption involving a chemical reaction between the adsorbate and the adsorbent. So this type of adsorption depends on the chemical properties of gas and the adsorbent [34].

Desorption is a phenomenon that a substance is released from the surface or through the surface. The process is the opposite of adsorption. This occurs in a system being in the state of sorption equilibrium between bulk phase and an adsorbing surface (solid or boundary separating two fluids). When the concentration (or pressure) of substance in the bulk phase is lowered, some of the sorbed substance changes to the bulk state [35,36].

An adsorbed species present on a surface at low temperatures may remain almost indefinitely in that state. As the temperature of the substrate is increased, however, a molecular species may decompose to yield either gas phase products or other surface species. An atomic adsorbate may react with the substrate to yield a specific surface compound, or diffuse into the bulk of the underlying solid and the species may desorb from the surface and return into the gas phase.

The last of these options is the desorption process. In the absence of decomposition, the desorbing species will generally be the same as that originally adsorbed but this is not necessarily always the case [37].

2.7 Literature reviews

Chung-Kung Lee et al [38] have reported that titanate nanotubes can absorb VOCs such as hexane, benzene toluene, p-xylene, m-xylene, and o-xylene. In this study, they synthesized titanate nanotubes from the reaction between TiO_2 powder and 10 M NaOH solution under a hydrothermal environment at 150 °C for 24 h. Next, it is washed with HCl aqueous solution of different concentrations (0.00001-0.1 mol/dm^3). It was found that titanate nanotubes washed with 0.01 mol/dm^3 HCl aqueous solution shows the highest adsorption capacity, due to the highest specific surface area and pore volume.

Audrey Maudhuit et al [39] used commercial titanium dioxide (TiO_2) as the adsorbent in adsorption of VOCs such as toluene, acetone and heptane. It was found that the adsorption of acetone is highest, followed by toluene and heptane.

Ikuo Ushiki et al [40] studied mesoporous MCM-41 as the adsorbent for VOCs such as acetone, toluene. The polar nature of MCM-41 results in the increasing efficiency of adsorption. This study demonstrates that the adsorption depends on the interaction between the adsorbent and adsorbate, and that the presence of charges at the adsorbent might be useful for adsorption.

Fang Qu. [41] studied the use of porous clay heterostructures (PCH) for the adsorption of VOCs. It was synthesized by modifying bentonite (Bent) with cetyltrimethyl ammonium bromide (CTMAB) and dodecylamine (DDA). VOCs studied include acetone, toluene, ethylbenzene, o-xylene, m-xylene and p-xylene.

Naoto Takahashi [42] studied the desorption behavior of five volatile organic compounds such as acetone, n-hexane, methanol, toluene, and n-decane from activated carbon by using supercritical carbon dioxide regeneration. The studied demonstrated that desorption behavior depended on the VOCs species, temperature and the pressure condition which explained the relation of the absorbent and CO_2 density.

Shufeng Zuo [43] studied volatile organic compound on Na-montmorillonite, Al and AlCe pillared clays supported Pd catalysts. They use nitrogen physisorption to determined specific surfsce areas (S_{BET}), mesopore volume (V_{meso}) and micropore volume (V_{micro}) of samples and use Temperature-programmed desorption of NH_3 (NH_3-TPD). The results show that after pillaring, S_{BET} and pore volume were obviously increased. And, increasing the S_{BET} and pore volume would improve the dispersion of Pd. In addition they suggest that catalysts with high S_{BET}, large pore volume and suitable acidity can adsorb more VOCs and this is the key factor to enhance catalytic activity for VOC deep oxidation.

Jiang Xu [44] studied the desorption of acetone on alkaline-earth exchange Y zeolite after room-temperature propane selective oxidation by in-situ infrared and mass spectroscopy. The intermediate product, isopropylhydroperoxide (IHP), did not desorb during temperature-programmed-desorption experiments but converted into acetone and water. The result of TPD shows that the CaY zeolite has two acetone adsorption sites, which they tentatively assign to Bro¨nsted acid sites and Ca(OH)*x* species. Acetone mainly desorbs at higher temperatures (>250 °C) under dry conditions. Addition of water results in have 2 desorption peaks shifting to lower temperature and show increased intensities. It can be concluded that water clearly facilitates acetone desorption, most likely via shielding of the electrostatic field and creation of additional sites.

Chapter 3

EXPERIMENTAL DETAILS

3.1 Reagents

1. Titanium dioxide (Carlo Erba), 98.5%
2. Potassium carbonate (Carlo Erba), 99%
3. Zinc oxide (Nano Materials Technology Co., Ltd.)
4. Sodium carbonate (Carlo Erba), 99%
5. Potassium chloride (Carlo Erba), 99%
6. Tetramethylammonium hydroxide [$(CH_3)_4NOH$] in water, 25wt% (Acrosorganics)
7. Tetrabutylammonium hydroxide [$(C_4H_9)_4NOH$] in water, 1 M (Fluka)
8. Hydrochloric acid, concentrated (Carlo Erba), ≥37 %
9. Sodium hydroxide anhydrous pallet (Carlo Erba)
10. Acetic acid glacial (Carlo Erba) 99.9%
11. Acetone (Carlo Erba) 99.8%
12. Acetonitrile (Carlo Erba) 99%
13. P25 TiO_2 nanopowder (TOA)

3.2 Apparatus

1. X-ray powder diffractometer (Rigaku, DMAX 2200/Ultima+, Faculty of Science, Chulalongkorn University)
2. Thermogravimetric analyzer (Perkin-Elmer, Scientific Instrument Service Centre, KMITL)
3. UV-visible spectrophotometer (T60, Bangkok High LAB Co., Ltd., Scientific Instrumental Service Centre, KMITL)

3.3 Experimental procedure

3.3.1 Preparation of adsorbents

3.3.1.1 Solid state synthesis of alkali titanates

Lepidocrocite titanate $K_{0.8}Zn_{0.4}Ti_{1.6}O_4$ "KZn" was prepared from a stoichiometric mixture of 8.3719 g K_2CO_3, 4.9378 g ZnO and 19.3771 g TiO_2 as reported previously [2]. The powder was ground together and then heated at 800°C for 1 hour, followed by a natural cooling down to room temperature. The mixture was reground before being heated at 900°C for another 20 hours.

Sodium trititanate ($Na_2Ti_3O_7$) was prepared from a stoichiometric mixture of 7.7319 g Na_2CO_3 and 15.8897 TiO_2 following the reported method [45]. The mixture was ground and then heated at 800°C for 40 hours, with the intermediate regrinding at every 20 hours.

3.3.1.2 Proton exchange/ Exfoliation/ Reassembled of lepidocrocite titanate KZn

Potassium ions in lepidocrocite titanate KZn were replaced by protons in the process called proton exchange [2]. The lepidocrocite titanate KZn powder was magnetically stirred with 1M HCl for 3 days (ratio of 1 g solid to 100 mL solution). The acid was renewed every day. After that the solid was filtered, washed by deionized water, and dried at room temperature.

An amount 0.4 g of the protonated lepidocrocite was exfoliated with tetrabutylammonium hydroxide (TBAOH). The mole ratio of TBA^+ cation in the solution to that of proton in the solid equals 1. The mixture was mechanically shaken at 180 rpm for 14 days. Then, the mixture was restacked by the dropwise addition of 400 mL of 1 M KCl. After that, the precipitates were washed with deionized water until free from excess TBAOH, as checked by the pH measurement. It was dried in the oven overnight at 100°C, and calcined at 450°C first for 2 hours, and then for another 4 hours, giving "K-rKZn". The reassembling with $BaCl_2$ gives "Ba-rKZn".

The exfoliation of $Na_2Ti_3O_7$ was attempted as well. $H_2Ti_3O_7$ was obtained from the proton exchange of $Na_2Ti_3O_7$ by the method similar to that with lepidocrocite titanate KZn. In the first method of exfoliation, an amount 0.4 g of $H_2Ti_3O_7$ was mechanically shaken with TMAOH. The molar ratio of TMA^+ cation in the solution to that of proton in the solid are 0.5, 1 and 5. The mixture was mechanically shaken at 180 rpm for 14 days. In the second exfoliation method, an amount of 1.5 g of $H_2Ti_3O_7$ was put into contact with TMAOH (also at TMA^+/H^+ = 0.5, 1 and 5). Then, the mixture was transferred to a teflon- lined autoclave and heated at 120°C for 4 hours. The precipitates were filtered and washed with deionized water until pH 7. In both cases, the samples were dried at room temperature.

3.3.1.3 Hydrothermal synthesis of Na-TNW and Na-TNT

The sodium titanate nanowire (Na-TNW) was prepared hydrothermally [23]. An amount of 0.5 g of P25 nanopowder was mixed with 50 mL of 10 M NaOH aqueous solution. The solution was stirred for 10 minutes before the transfer into a Teflon-lined autoclave. The mixture was heated at 150°C for 10 hours. Then, the precipitates were washed with 0.1 M HCl and deionzied water until pH 7. The sample was dried at 40°C overnight.

Sodium titanate nanotube (Na-TNT) was also synthesized by a hydrothermal method, by another member of this laboratory.

3.3.2 Characterization

3.3.2.1 Structural analysis using X-ray diffraction (XRD)

The crystalline phase of the materials prepared can be identified using XRD measurement. The sample was ground before it was packed on the sample holder. Analysis was done employing the Bruker diffractometer (Cu K α radiation, 40 kV, 30 mA), covering the range 2θ = 5-65 ° and 2θ = 5-80°, at the rate of 0.02 ° /step and a scanning rate of 0.6 s/step.

3.3.2.2 Thermogravimetric analysis (TGA)

The mass loss of the sample after being heated to a high temperature was recorded by a Perkin-Elmer thermogravimetric analyzer. Approximately 10-20 mg of the powder was loaded to the platinum pan, after which the exact mass was read by the instrument. The sample was then heated from room temperature to 900°C at the heating rate of 10°C/min under the flow of nitrogen gas (40 mL/min). The mass of the powder was recorded as a function of time and temperature.

3.3.2.3 Light absorption by UV-Vis spectroscopy

The absorption spectra of the suspensions (from the exfoliation) were recorded by a UV-vis spectrophotometer. DI water was used as the reference solution for baseline correction. The suspension with the nominal concentration of 4 g/L was diluted to a concentration of 0.08 g/L with deionized water. Subsequently, the solution was filled into a quartz cuvette, thus enabling the recording of the spectrum down to the UV region. The wavelength was scanned from 200 to 900 nm.

3.3.4 Adsorption and desorption of VOCs

The nanomaterials to be tested as absorbent were pressed, crushed, and sieved to a size of 600-850 μm. An amount of 0.1 g of sieved material was packed into the quart tube and both the top and the bottom part were next covered by quart wool. The schematic diagram of the adsorption system is shown in **Figure 3.1**. The quart tube has the outer diameter of 8 mm, inner diameter of 6 mm and the length of 50 cm. Before adsorption measurement, the absorbent was activated by heating from 50 to 450 °C following by the holding at 450 °C for 2 hours for lepidocrocite titanate KZn, the K-rKZn and Ba-rKZn made from lepidocrocite titanate KZn, Na-TNW and commercial P25 TiO_2. The activation of Na-TNT and Ba-TNT was done similarly but using the temperature of 300 °C. The heating rate employed was 5 C°/min, and air zero was used throughout the activation. The flow rate of air zero was controlled by a rotameter and was checked by a bubble flow meter. Then, nitrogen gas (30 mL/min) was passed from the saturator containing the vapor of acetone (or acetonitrile) through the adsorption bed inside the quartz tube. The total adsorption time is of 30 min. During adsorption, the temperature at the furnace was set at 50 °C. Then, the nanomaterials pre-adsorbed with selected VOCs were purged with nitrogen gas (30 mL/min) for 1 hour to remove weakly-sorbed molecules. Next, the pre-adsorbed VOCs were desorbed by a temperature-programmed desorption (TPD) technique as follows. The temperature at the bed was increased (10 °C/min) from 50 to 900 °C, while He gas was flown through the bed (30 mL/min, controlled by a mass flow controller). The signal was recorded using the TCD detector.

The conversion of the peak area from TCD into the amount adsorbed in mmol was performed as follows. He gas was continuously flown through the tube (30 mL/min, controlled by a mass flow controller) at the temperature of 50 °C. Next, an amount of 0.1 μL of acetone (or acetonitrile) was injected via the injection port of the TCD detector. The peak area obtained was then used for further calculations. In this work, the peak area of acetone of 0.4119 units equals 0.0013 mmol, and the peak area of acetonitrile of 0.6209 units equals 0.0018 mmol.

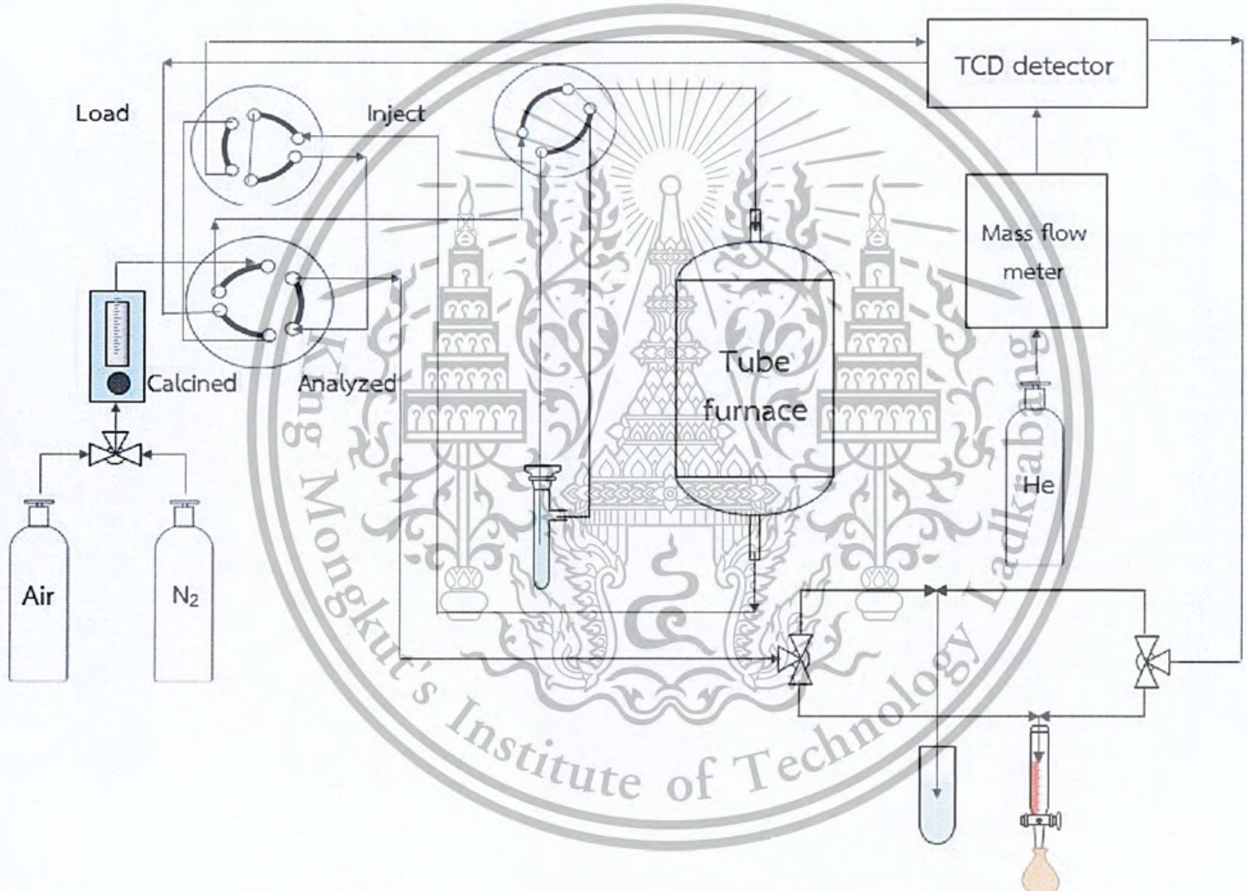

Figure 3.1 Schematic diagram of the VOCs adsorption measurement.

CHAPTER 4

RESULTS AND DISCUSSION

4.1. Solid state synthesis

Lepidocrocite titanate KZn was successfully prepared by the solid state synthesis as described in **Chapter 3**. The sharp peaks in the PXRD pattern shown in **Figure 4.1(a)** are in reasonable agreement with those reported in [46]. The absence of peaks due to other phase(s) suggests that there is no crystalline impurity. The first peak at 2θ= 11.3° (d = 0.7859 nm) refers to the 020 reflection, which is the repeating distance between sheets along the *b*-direction of the orthorhombic unit cell.

The $Na_2Ti_3O_7$ can also be synthesized similarly. Its PXRD pattern shown in **Figure 4.1(b)** is similar to that reported in the literature [45], thereby confirming the successful synthesis of $Na_2Ti_3O_7$. The first peak at 2θ= 10.58° (d = 0.8385 nm) refers to the 001 reflection, which is the repeating distance between sheets along the *c*-direction of the monoclinic unit cell.

Na-TNW can be synthesized by a hydrothermal method as described in **Chapter 3**. The PXRD pattern shown in **Figure 4.1(c)** is also similar to that reported in literature [23]. Similarly, Na-TNT was obtained from members of this laboratory. The PXRD pattern in **Figure 4.1(d)** is similar to that reported in literature [47]. The similarity in the PXRD patterns of Na-TNW and Na-TNT suggests that these two products have the same crystal structure. The difference between them is the morphology. In both cases, the first peak is at 2θ = 9.7° (d =0.9151 nm), which is the 020 reflection of sheets stacked along the *b*-direction. The larger interlayer separation in Na-TNW and Na-TNT (d =0.9151 nm) in comparison to that of lepidocrocite titanate KZn (d = 0.7859 nm) could be ascribed to the presence of water molecules in the former.

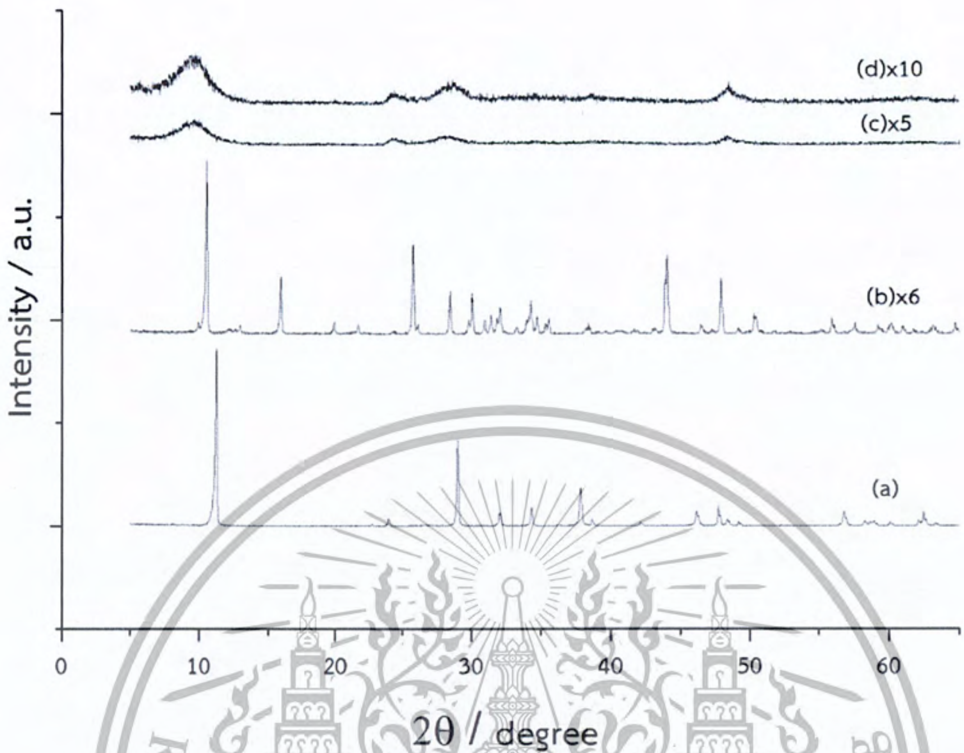

Figure 4.1 PXRD patterns for (a) lepidocrocite titanate KZn, (b) $Na_2Ti_3O_7$ (x6), (c) Na-TNW (x5), and (d) Na-TNT (x10).

4.2 Ion exchange

Lepidocrocite titanate KZn was prepared by solid state synthesis. Potassium ions in lepidocrocite titanate KZn were replaced with protons of HCl via proton exchange process. However, not only proton has been exchanged. The framework Zn was also leached. The structural composition of the product after proton exchange will be then referred to as "$H_{1.6}\square_{0.4}Ti_{1.6}O_4{\bullet}0.8H_2O$". **Figure 4.2** shows the mass loss curve of $H_{1.6}\square_{0.4}Ti_{1.6}O_4{\bullet}0.8H_2O$. Similar to the previous report [2], two regions of the mass loss can be observed. The first region is from 50 to 110°C (10.00%) and the second region is from 120 to 500°C (9.50%). For proton-containing lepidocrocite titanate KZn, the first mass loss [2] is explained as the release of water molecules between the layers, while the second mass loss is due to the condensation of the OH groups resulting in the collapse of the layers. These two steps are shown in equation 4.1 (theoretical mass loss 9.21%) and 4.2 (theoretical mass loss, also at 9.21%).

$$H_{1.6}\square_{0.4}Ti_{1.6}O_4{\cdot}0.8H_2O\ (s) \rightarrow H_{1.6}\square_{0.4}Ti_{1.6}O_4\ (s) + 0.8H_2O\ (g) \quad (Eq.4.1)$$

$$H_{1.6}\square_{0.4}Ti_{1.6}O_4\ (s) + 0.4O_2\ (g) \rightarrow 2Ti_{0.8}\square_{0.2}O_2 + 0.8H_2O\ (g) \quad (Eq.4.2)$$

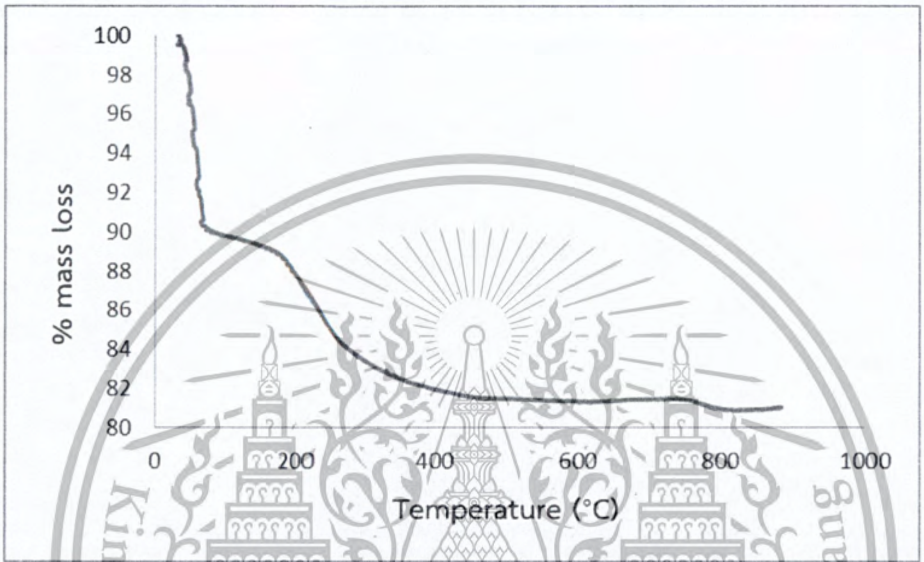

Figure 4.2 Mass loss curve of $H_{1.6}\square_{0.4}Ti_{1.6}O_4{\cdot}0.8H_2O$

$Na_2Ti_3O_7$ was prepared by solid state synthesis. Sodium ions in $Na_2Ti_3O_7$ were replaced with protons of HCl via proton exchange process. The product from the proton exchange of $Na_2Ti_3O_7$ will be here after called "$H_2Ti_3O_7$". The PXRD pattern of $H_2Ti_3O_7$ shown in **Figure 4.3** is in agreement with the literature. The first peak of $H_3Ti_2O_7$ is now at 2θ = 11.26° (d = 0.7682 nm) and is assigned as the 001 reflection. This value indicates a shrinking of the interlayer distance along the *c*-direction upon proton exchange due to the smaller size of protons compared to sodium cations. Hence, these results indicate the successful ion exchange of $Na_2Ti_3O_7$ into $H_2Ti_3O_7$.

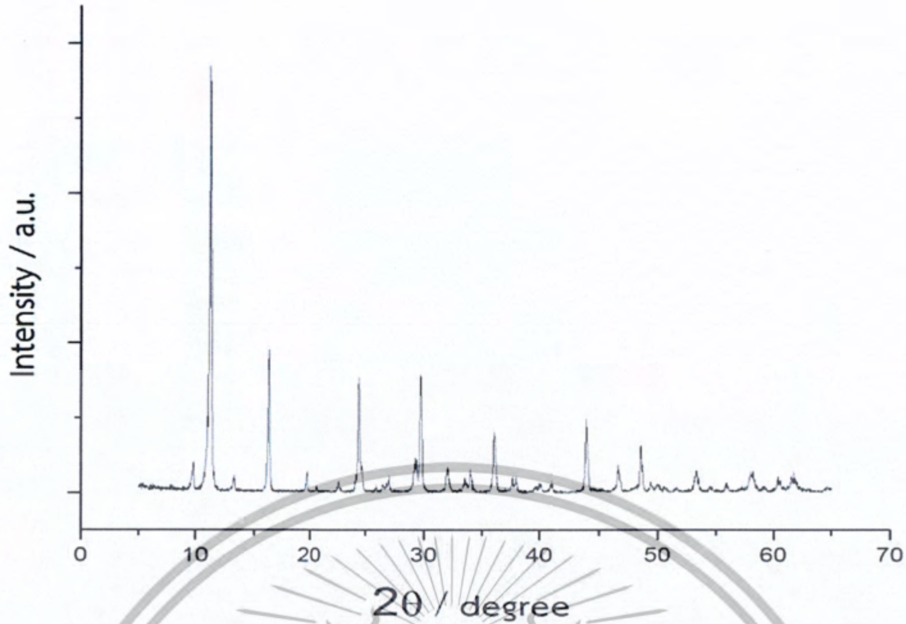

Figure 4.3 PXRD patterns for $H_2Ti_3O_7$

The TGA mass loss curve of $H_2Ti_3O_7$ is shown in **Figure 4.4**. Only one step of the mass loss was observed (6.77%) from 210 to 390 °C follow in equation 4.3.

$$H_2Ti_3O_7\,(s) \longrightarrow 3TiO_2 + H_2O\,(g) \qquad \text{(Eq.4.3)}$$

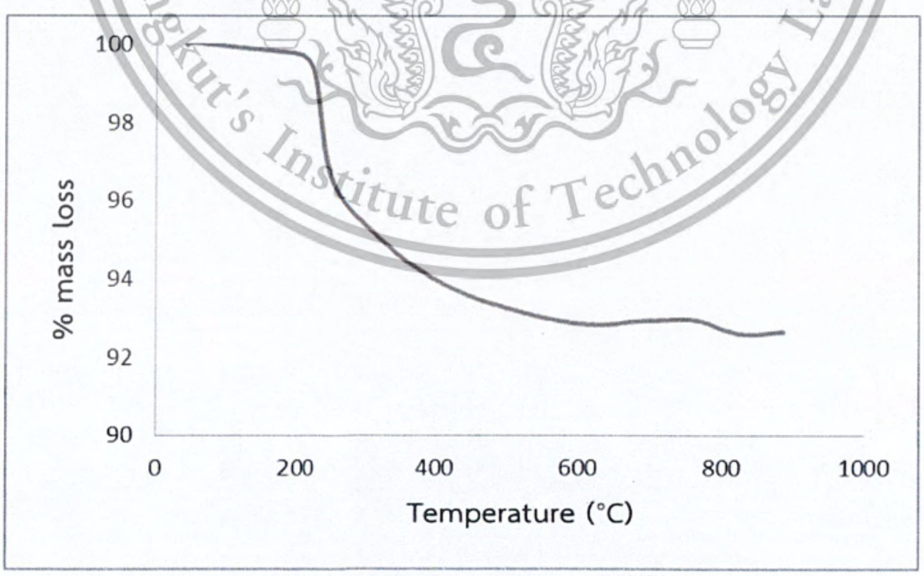

Figure 4.4 Mass loss curve of $H_2Ti_3O_7$

4.3 Exfoliation of $H_{1.6}\square_{0.4}Ti_{1.6}O_4$•$0.8H_2O$ and $H_2Ti_3O_7$

Exfoliation of $H_{1.6}\square_{0.4}Ti_{1.6}O_4$•$0.8H_2O$ into individual elementary layers was accomplished by the mechanical shaking of $H_{1.6}\square_{0.4}Ti_{1.6}O_4$•$0.8H_2O$ with TBAOH (180 rpm) for 14 days. The product from the ion exchange $H_{1.6}\square_{0.4}Ti_{1.6}O_4$•$0.8H_2O$ of will be here after called "$H_{1.6}\square_{0.4}Ti_{1.6}O_4$•$TBA^+$" The molar ratio of TBA^+ in the solution to H^+in the solid to is fixed at 1.0. During the reaction, the starting mixture containing white powder and clear, colorless TBAOH liquid gradually changed into a white suspension. After the exfoliation, the Tyndall effect of the suspension can be clearly observed as shown in the inset of **Figure 4.5**. Such a colloidal suspension indicates the separation of stacks of titanate layers into individual, elementary layers known as nanosheets [2]. Hence, it can be inferred that $H_{1.6}\square_{0.4}Ti_{1.6}O_4$•$0.8H_2O$ was exfoliated into individual layers in the reaction of TBAOH exchange. The obtained suspension at the nominal concentration of 4 g/L was diluted to a concentration of 0.008 g/L before analysis by UV-VIS spectroscopy. As shown in **Figure 4.5** the suspension showed λ_{max} at 262 nm in agreement with the previous report [2].

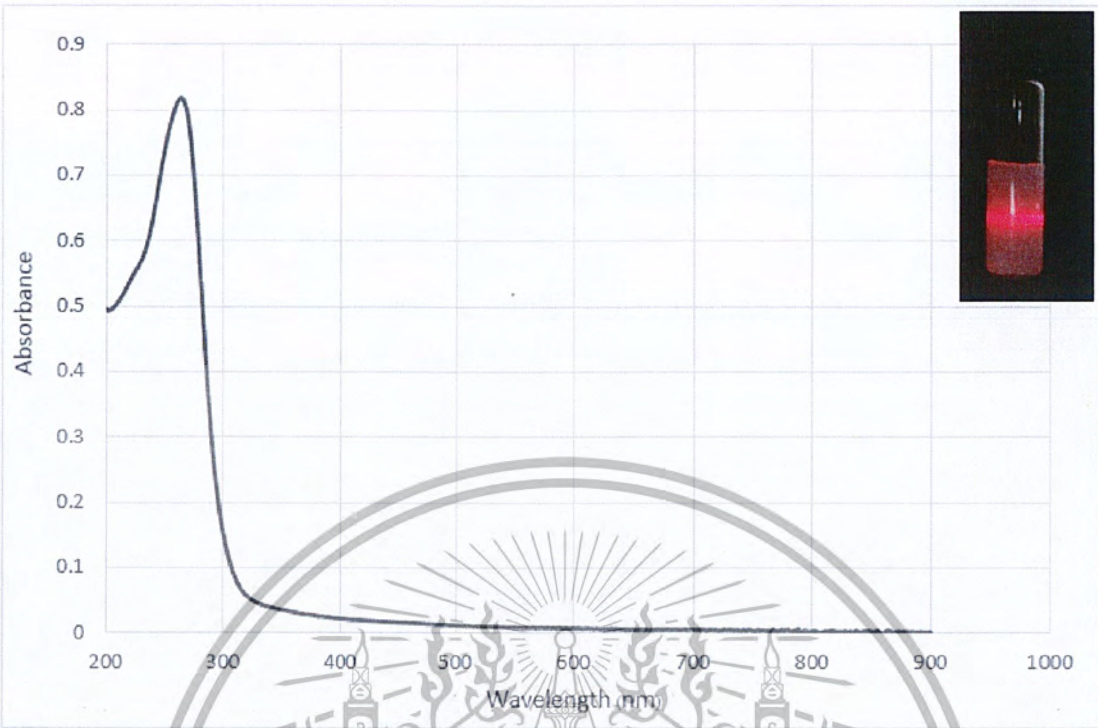

Figure 4.5 UV-visible absorption spectrum of the titanate suspension at a nominal concentration of 0.008 g/L, prepared from the mechanical shaking of the protonated form of $H_{1.6}\square_{0.4}Ti_{1.6}O_4{\cdot}0.8H_2O$ with TBAOH. The inset shows a representative photograph exhibiting the Tyndall effect.

The exfoliation of $H_2Ti_3O_7$ was also attempted at TMA^+/H^+ = 0.5, 1, 5. In the first method where $H_2Ti_3O_7$ was mechanically shaken with TMAOH for 14 days, the mixture did not change into colloid. The solid settled into the bottom of the flask when the shaking was stopped. The Tyndall effect could not be observed. Similarly, reaction under a hydrothermal condition did not give the colloid. One can conclude that the attraction between sheets $H_2Ti_3O_7$ is so strong that TMA^+ cannot penetrate into the layers. Hence, the exfoliation of $H_2Ti_3O_7$ by TMA^+ was not possible.

4.4 Reassembling of lepidocrocite titanate nanosheets

Reassembling was achieved by the dropwise addition 1 M KCl or $BaCl_2$ into the suspension containing exfoliated the reassembled $H_{1.6}\square_{0.4}Ti_{1.6}O_4 \cdot TBA^+$. By adding KCl or $BaCl_2$, the electrostatic attraction between K^+ (Ba^{2+}) cations and the negatively-charged nanosheets results in the reassembled $H_{1.6}\square_{0.4}Ti_{1.6}O_4 \cdot TBA^+$ likely with K^+ (Ba^{2+}) in between. This material will be called "reassembled $H_{1.6}\square_{0.4}Ti_{1.6}O_4 \cdot TBA^+$". It is a white powder similar to the parent lepidocrocite titanate KZn and $H_{1.6}\square_{0.4}Ti_{1.6}O_4 \cdot 0.8H_2O$ (proton form).

Thermogravimetric analysis of the reassembled $H_{1.6}\square_{0.4}Ti_{1.6}O_4 \cdot TBA^+$(**Figure 4.6**) shows 8.00% mass loss which is ascribed to the intercalated water molecules.

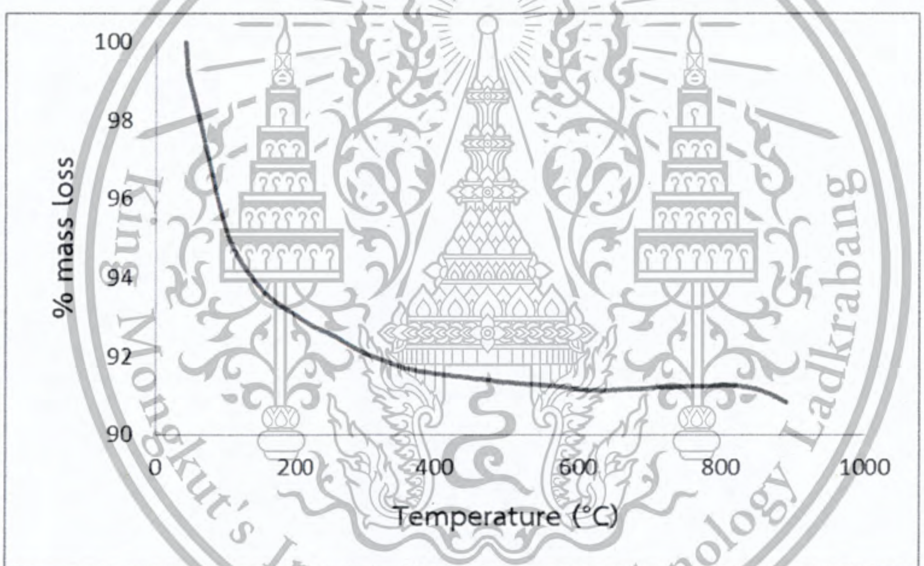

Figure 4.6 Mass loss curve of the reassembled $H_{1.6}\square_{0.4}Ti_{1.6}O_4 \cdot TBA^+$ with 1M KCl (K-rKZn)

This material as obtained, and after calcination at 450°C for 6 hours were characterized by PXRD. The PXRD pattern of the reassembled material before calcination shows the strongest peak at 9.62°, corresponding to d =0.9215 nm. This interlayer spacing is larger than that of the starting lepidocrocite titanate KZn (d = 0.7859 nm) and Na-TNW (d=0.9151 nm). Hence, it might be possible that hydrated potassium cations $K(H_2O)_n^+$ are occluded between the layers. In additions, other peaks at 2θ = 19.82°, 29.27°, 48.22° and 62.74° can be observed and correspond to *d* = 0.4541, 0.3150, 0.2065 and 0.1732 nm respectively. Altogether, these peaks in **Figure 4.7(a)** can be indexed (from left to right) as 010, 020, 030, 050 and 060 reflections. These results suggest the preferred orientation of the reassembled material along the *b*-direction, supporting the reassembled of the two-dimensional nanosheets.

Upon calcination, **Figure 4.7(b)** shows the new phase with the peaks at 2θ = 40.53°, 50.19° and 58.67° corresponding to d = 0.2370, 0.2005, and 0.1803 nm respectively. The peaks in **Figure 4.7(b)** can be indexed (from left to right) as the 110, 220, 210 and 220 reflection characteristics of rutile TiO_2. Moreover, the intensity is greatly increased as compared to that before calcination.

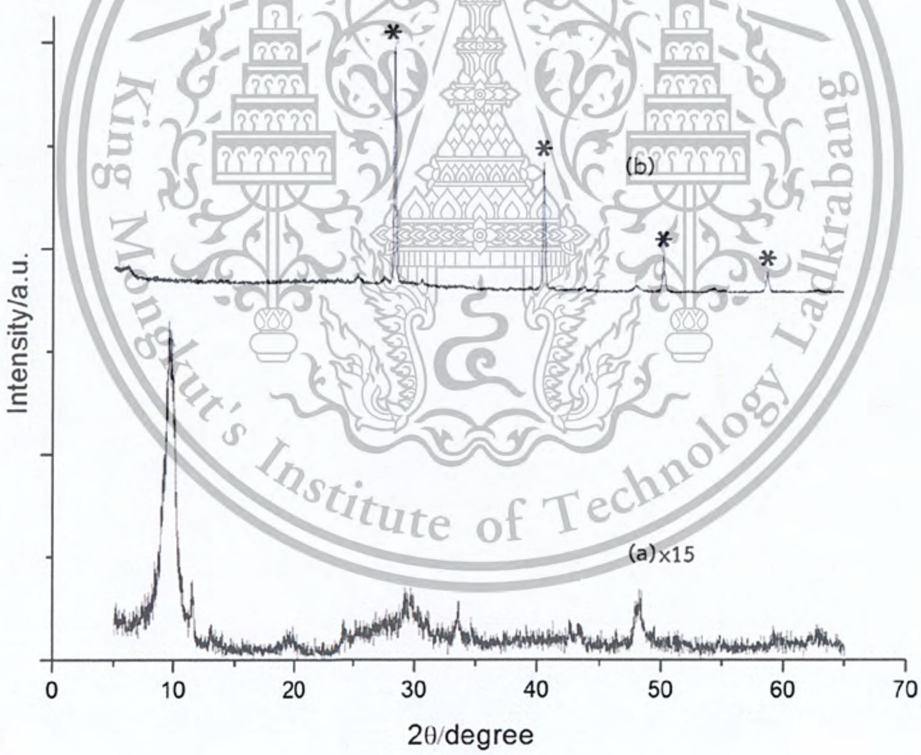

Figure 4.7 PXRD pattern for (a) as made K-rKZn from the suspension exfoliated with TBAOH, and (b) after the calcination at 450 °C 6 hours.

4.5 Textural properties

Table 4.1 summarizes the specific surface area of some titanate-based materials absorbent prepared. Lepidocrocite titanate KZn has low specific surface area of 3.1 m^2/g. After the exfoliation, reassembled with KCl, and calcination at 450 $^{\circ}C$ for 6 hours, an increase in the specific surface area to 27.7 m^2/g could be noticed. As we did not measure, the specific surface area of Na-TNW, we assume the value of 7.0 m^2/g as reported [23] in the literature. And, the specific surface area of commercial P25 TiO_2 is 53.0 m^2/g which is characterized by members in the laboratory. Na-TNT possess the largest specific surface area of 270.0 m^2/g.

Table4.1: Surface area of absorbents prepared.

Absorbent	Surface area (m^2/g)
Lepidocrocite titanate KZn	3.1
K-rKZn calcined at 450 $^{\circ}C$ 2 hours	27.7
Na-TNW	7.0 [23]
Na-TNT	270.0
Commercial P25 TiO_2	53.0

4.6 Desorption Testing

4.6.1 Study of the desorption of acetone

4.6.1.1 Desorption of acetone on lepidocrocite titanate KZn, the K-rKZn and Ba-rKZn

They were also tested for the adsorption/desorption of acetone. Lepidocrocite titanate KZn and the K-rKZn and Ba-rKZn was tested for the desorption of acetone. Results are shown in **Figure 4.8.**

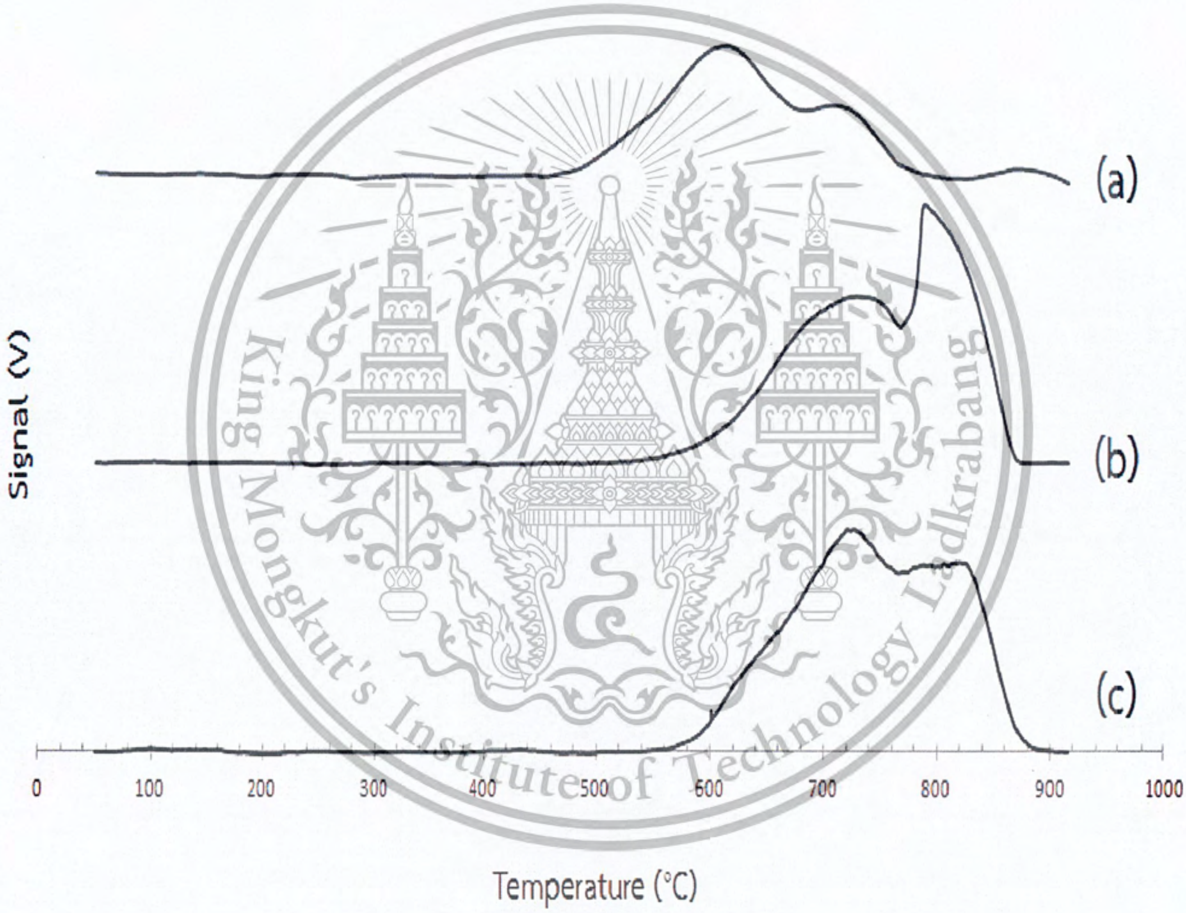

Figure 4.8 TPD profiles of acetone pre-adsorbed on nanomaterials absorbent: (a) lepidocrocite titanate KZn, (b) K-rKZn, and (c) Ba-rKZn

From **Figure 4.8** it can be seen that for lepidocrocite titanate KZn, the signals due to desorption were observed in the range 445-800°C. However, this is a very high desorption temperature (much higher than the boiling point of acetone, 56.53°C). Hence, it is unlikely that these signals are due to the desorption of acetone. We propose that these signals could be due to some volatile products from the decomposition of lepidocrocite titanate KZn structure after being heated at relatively high temperature (up to 800°C). The structure might collapse, although we do not have the proof at this moment. Similar results were obtained from K-rKZn and Ba-rKZn. The desorption temperature of 553-880°C was observed for the K-rKZn, and 534-900°C with Ba-rKZn. So, one can conclude that acetone cannot adsorb on lepidocrocite titanate KZn and the reassembled form.

4.6.1.2 Desorption of acetone on Na-TNW, Na-TNT, Ba-TNT and commercial P25 TiO_2

Na-TNW, as compared to Na-TNT, Ba-TNT and commercial P25 TiO_2 were tested for desorption of acetone using the temperature program desorption technique. The desorption profiles discussed above are all broad. Hence, in this section, a more quantitative comparison of the thermal desorption behavior was performed by peak deconvolution. Results are shown in **Figure 4.9** and in **Table 4.2**.

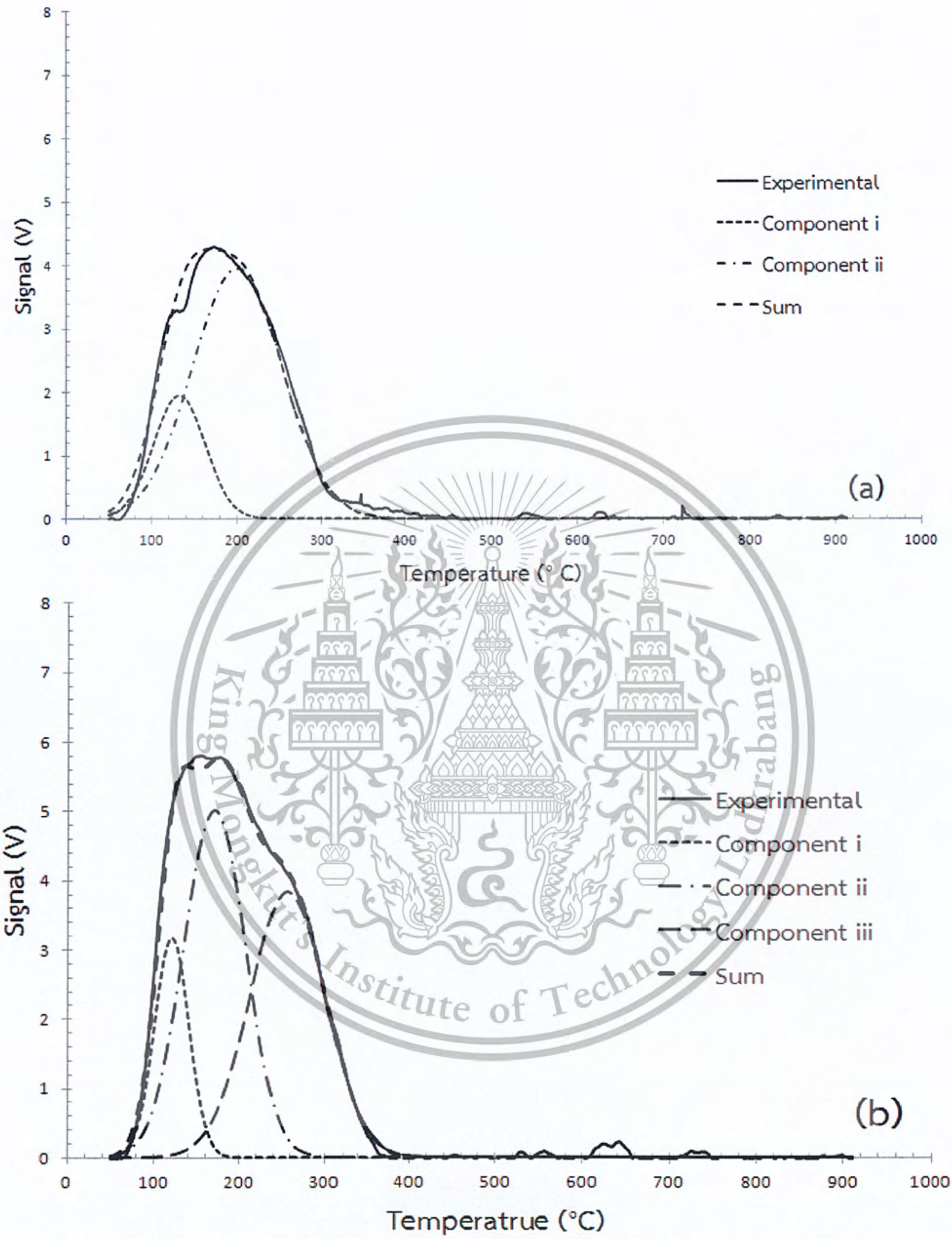

Figure 4.9 The deconvolution of TPD profile of acetone on several titanate-based materials: (a) Na-TNW, (b) Na-TNT, (c) Ba-TNT, and (d) commercial P25 TiO_2.

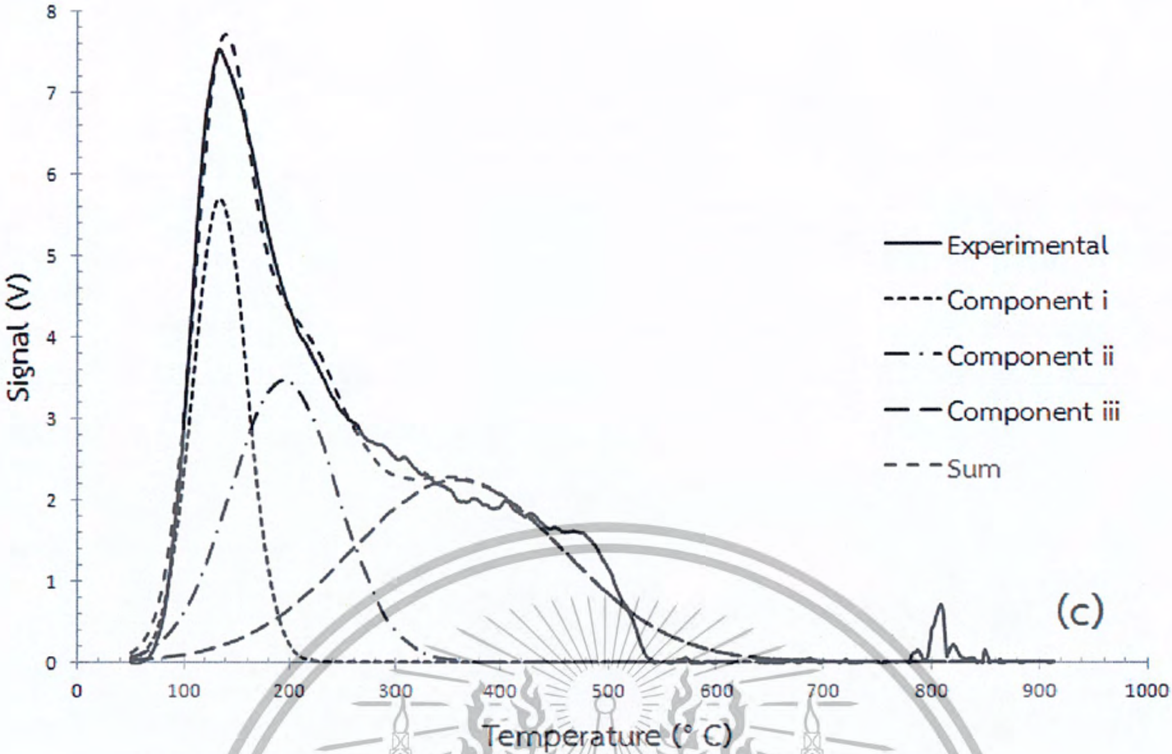

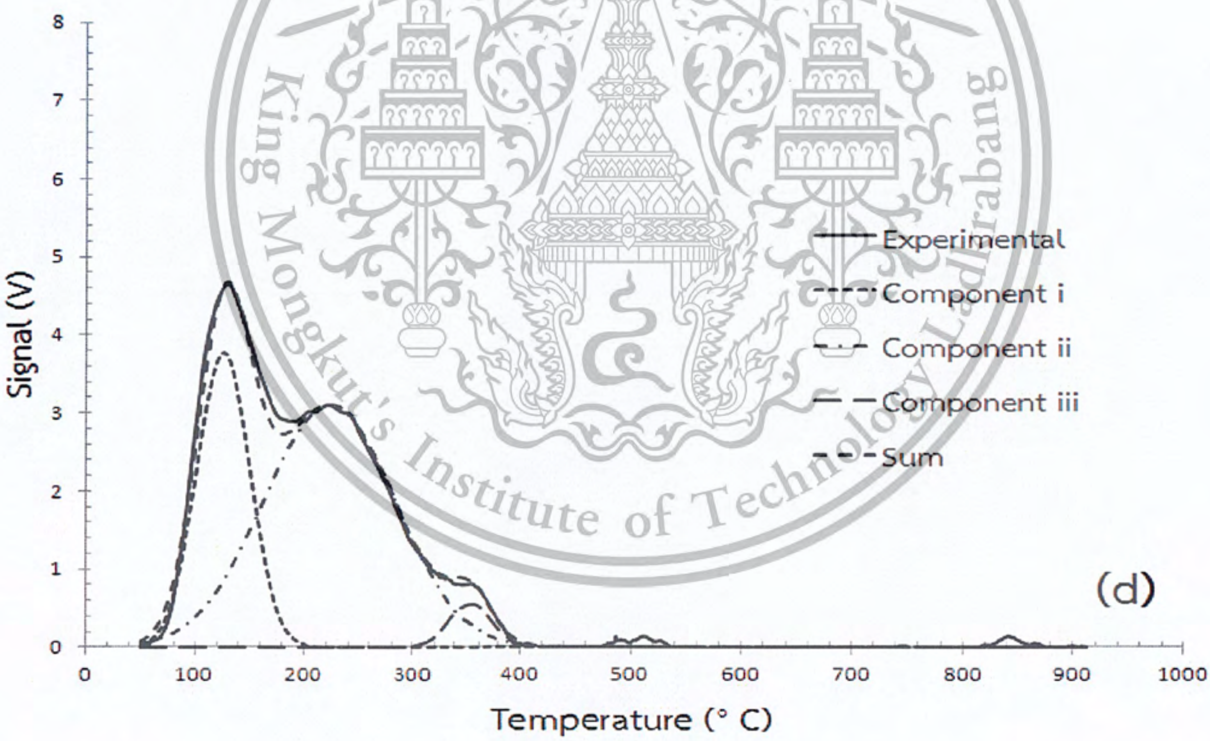

Figure 4.9(continued) The deconvolution of TPD profile of acetone on several titanate-based materials: (a) Na-TNW, (b) Na-TNT, (c) Ba-TNT, and (d) commercial P25 TiO_2.

The desorption of acetone on Na-TNW, Na- and Ba-TNT, and commercial P25 TiO_2 can be divided into three parts as summarized in Table 4.2.

<u>Table 4.2</u>: Summary of the deconvolution of the acetone-TPD profiles of several titanate-based materials

Adsorbent	Total mmol /g	Component i				Component ii				Component iii			
		$T_{initial}$	T_{peak}	T_{final}	mmol/g	$T_{initial}$	T_{peak}	T_{final}	mmol/g	$T_{initial}$	T_{peak}	T_{final}	mmol/g
Na-TNW	2.0	50°C	137°C	227°C	0.4	50°C	201°C	365°C	1.6	-	-	-	-
Na-TNT	3.2	50°C	118°C	171°C	0.5	50°C	167°C	277°C	1.4	121°C	255°C	376°C	1.3
Ba-TNT	4.0	50°C	133°C	222°C	1.1	50°C	191°C	351°C	1.1	50°C	367°C	534°C	1.8
Commercial P25 TiO_2	2.2	50°C	124°C	200°C	0.7	61°C	217°C	385°C	1.4	300°C	353°C	396°C	0.1

In Figure 4.9(a), it was found that that Na-TNW desorbs acetone in the temperature range 50-365 °C (2.51 mmol/g). Na-TNT in Figure **4.9(b),** Ba-TNT in **Figure4.9(c)** (synthesized by other members in this laboratory) and the commercial P25 TiO_2 **in Figure 4.9(d)** were tested as adsorbents for acetone. It was found that acetone desorbed from Na-TNT in the range 50-376 °C (3.93 mmol/g), from Ba-TNT in the range 50-534 °C (4.85 mmol/g) and the commercial P25 desorbed acetone in the range of 50-396 °C (2.75 mmol/g). This amount of desorbed acetone is less than that of two samples of the titanate nanotubes and commercial P25 TiO_2 mentioned above. Na-TNW is not hollow but instead dense. According to some literature review [23], a low surface area approximately of 7.0 m^2/g was reported. The low desorption temperature of acetone on Na-TNW, as compared to three other materials suggest that the interactions between Na-TNT and acetone are weaker than those between the three nanostructured absorbents and acetone.

The larger amount of desorbed acetone in these TNT (3.93-4.85 mmol/g), as compared to Na-TNW (2.51 mmol/g) and commercial P25 TiO_2 (2.75 mmol/g) could be due to their relatively high surface area, as reported by several authors [47]. Titanate nanotube is long and hollow objects. This nanostructure might allow the interaction with acetone molecules both at the internal and the external surfaces. In particular, titanate nanotube ion exchanged with $BaCl_2$ desorbed acetone molecules at temperature (367 °C) higher than that of the Na-TNT (255 °C) and commercial P25 TiO_2 (353 °C). These results might be explained considering that Ba^{2+} has higher charge, as compared to Na^+. Hence, the interactions of Ba^{2+} with acetone should be stronger than those of Na^+ and acetone.

The first component desorbing at 118-137 °C, likely represents acetone molecules having weak interactions with the surfaces of the materials, i.e. physisorption at external surface. The second component (component ii) has the peak temperature around 167-217 °C. This peak could be ascribed to the desorption of chemisorbed acetone as shown in **Scheme 4.1.**

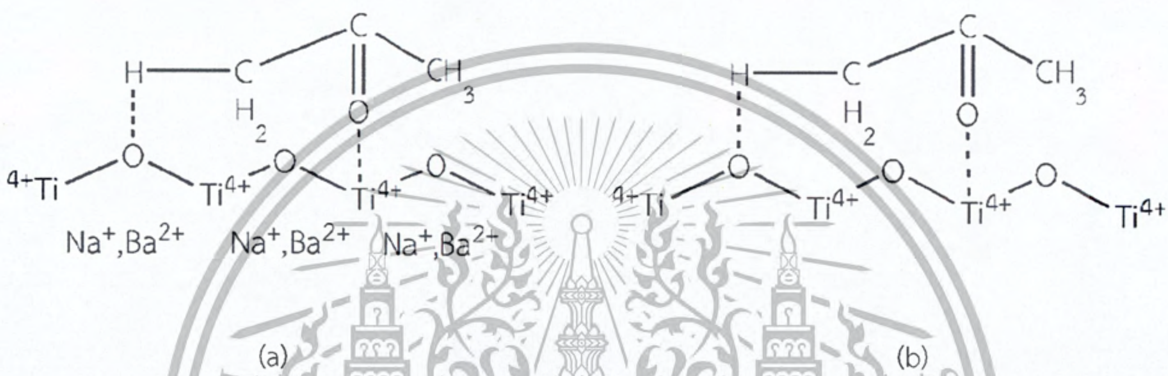

Scheme 4.1 Schematic illustration of the chemisorption showing the interactions of an acetone molecule with the surfaces of (a) Na-TNW, Na-TNT and, Ba-TNT (b) commercial P25 TiO_2.

Finally, the last component (component iii) is in the range 255-367 °C. This component might be the product from the condensation of acetone at basic site as shown **Scheme 4.2.**

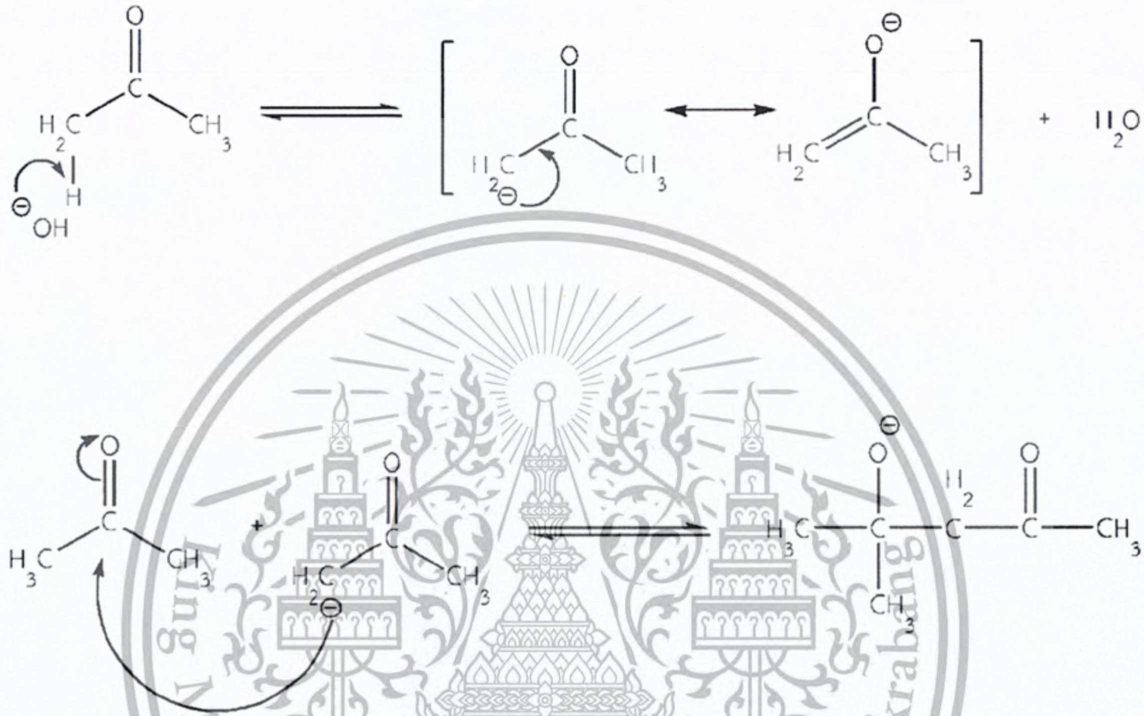

Scheme 4.2 Proposed reaction mechanism for the condensation of acetone at basic sites in TNT and commercial P25 TiO_2.

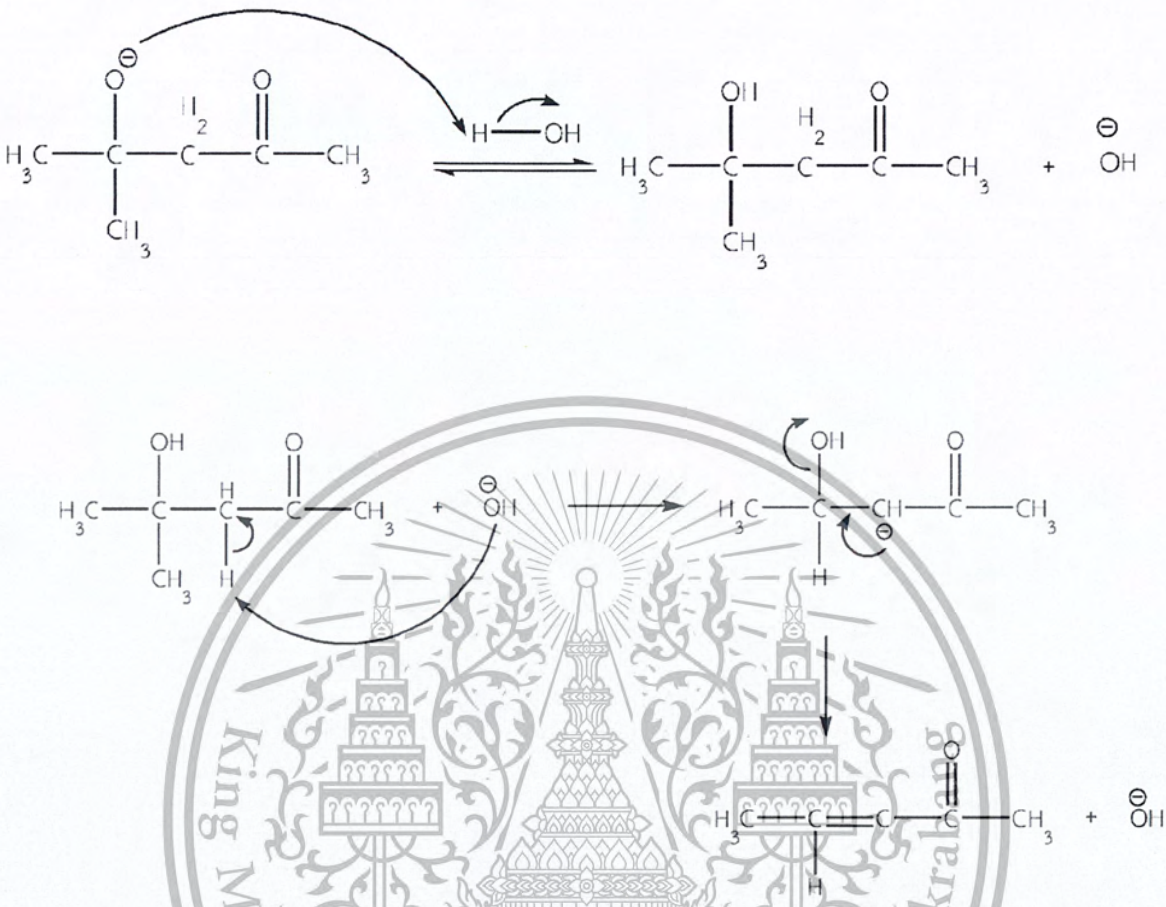

Scheme 4.2 (continued) Proposed reaction mechanism for the condensation of acetone at basic sites in TNT and commercial P25 TiO_2.

Na-TNW shows mostly chemisorption on acetone with no condensation product. This result might be because it retains rutile structure that contains less number of defects.

The majority of the desorbed species on Na- and Ba-TNT appears at high temperature **(Figure 4.9(b) and (c))**. These suggest that the titanate nanotubes process a large number of basic sites that promote aldol condensation of acetone. On Ba-TNT, the product from the condensation of acetone is higher than that from Na-TNT. These results might be explained considering that Ba^{2+} is more basic than Na^{+}. This is because Ba^{2+} is larger and processes lower charge density, as compared to Na^{+}.

Over commercial P25 TiO_2, the larger fraction of desorbed acetone is at the medium temperature and the minority is at high temperature, as shown in **Figure 4.9** (d). Hence, it is suggested that acetone processes strong interaction with the surface and some undergo aldol condensation.

4.6.2. Study of desorption of acetonitrile

4.6.2.1 Desorption of acetonitrile on on Na-TNW, Na TNT, Ba-TNT and commercial P25 TiO_2

The desorption profiles discussed above are all broad. It was found that lepidocrocite titanate KZn and the K-rKZn and Ba-rKZn as these samples do not show any desorption peaks of acetone.

Na-TNW, as compared to Na-TNT, Ba-TNT and commercial P25 TiO_2 were also tested for desorption of acetonitrile using the temperature desorption program technique. Results are shown in **Figure 4.10** and in **Table 4.3**.

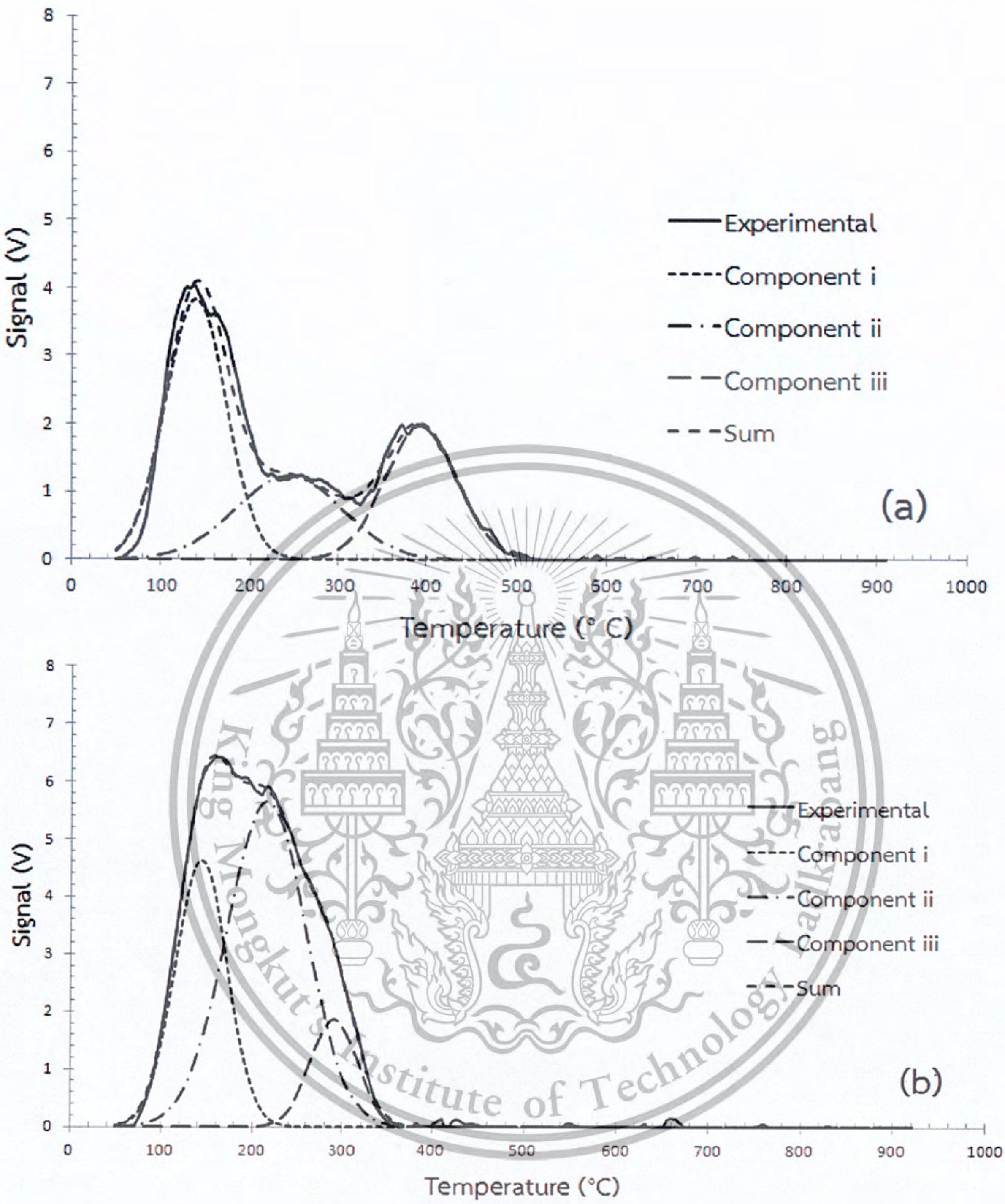

Figure 4.10 The deconvolution of TPD profile of acetonitrile on several titanate-based materials: (a) Na-TNW, (b) Na-TNT, (c) Ba-TNT, and (d) commercial P25 TiO_2.

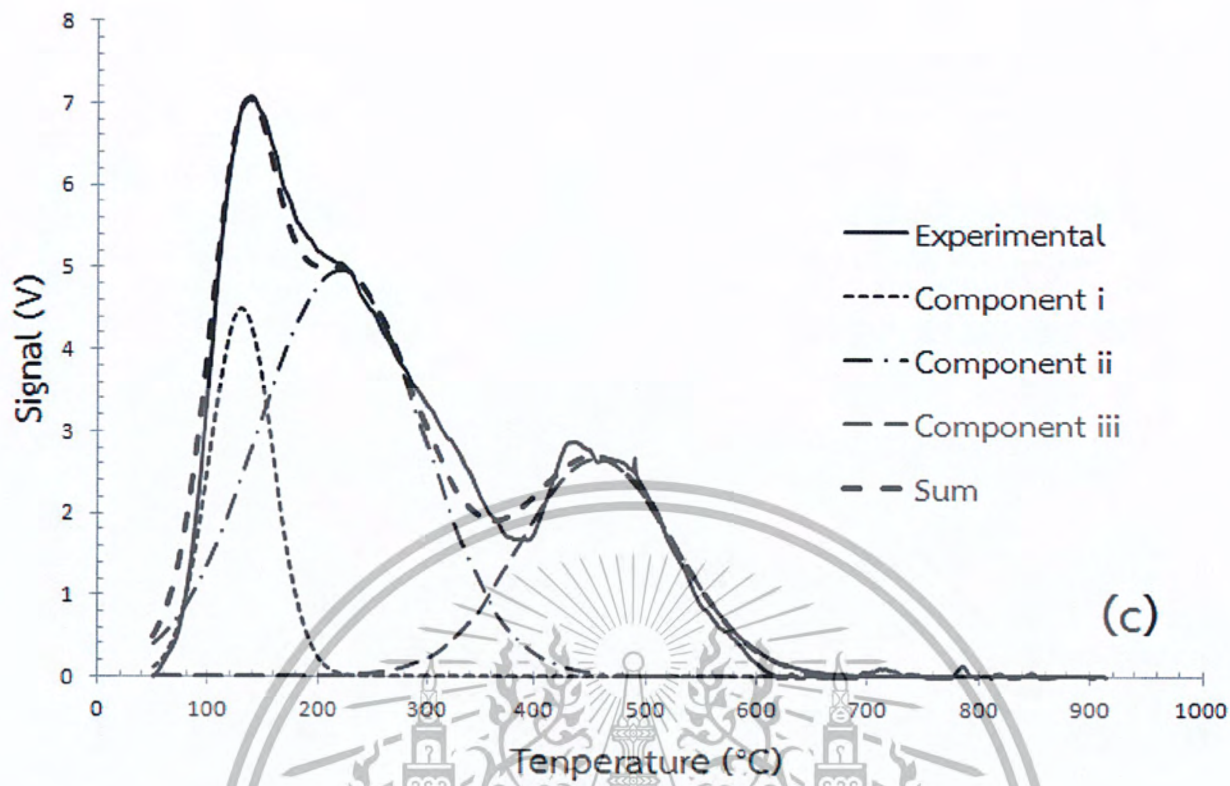

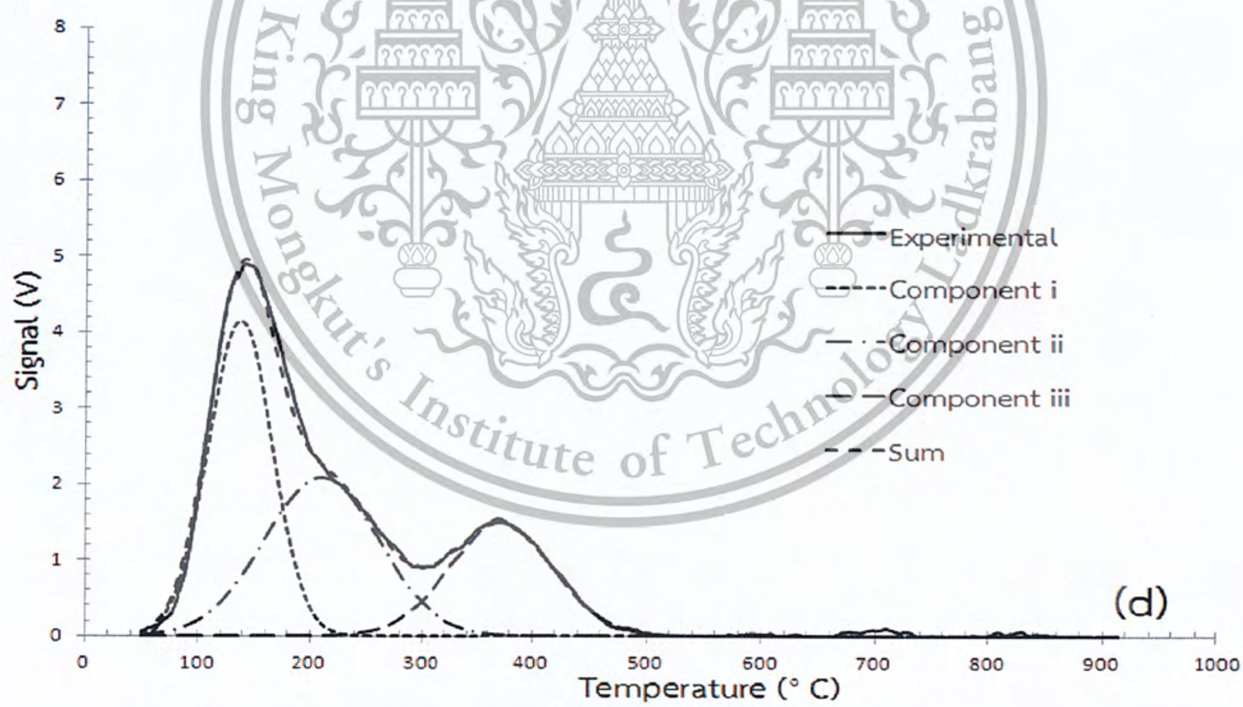

Figure 4.10 (continued) The deconvolution of TPD profile of acetonitrile on several titanate-based materials: (a) Na-TNW, (b) Na-TNT, (c) Ba-TNT, and (d) commercial P25 TiO_2.

The desorption of acetonitrile on Na-TNW, Na- and Ba-TNT, and commercial P25 TiO_2 can also be divided into three parts as summarized in Table 4.3.

Table4.3: Summary of the deconvolution of the acetonitrile-TPD profiles of several titanate-based materials

Adsorbent	Total mmol /g	Component i				Component ii				Component iii			
		$T_{initial}$	T_{peak}	T_{final}	mmol/g	$T_{initial}$	T_{peak}	T_{final}	mmol/g	$T_{initial}$	T_{peak}	T_{final}	mmol/g
Na-TNW	2.2	50°C	139°C	236°C	1.0	107°C	244°C	385°C	0.6	272°C	391°C	520°C	0.6
Na-TNT	3.2	50°C	143°C	236°C	1.0	72°C	215°C	346°C	1.8	215°C	283°C	360°C	0.4
Ba-TNT	5.3	50°C	130°C	215°C	1.0	50°C	220°C	452°C	2.9	265°C	457°C	645°C	1.4
Commercial P25 TiO_2	2.2	50°C	135°C	218°C	0.9	65°C	210°C	351°C	0.8	233°C	360°C	500°C	0.5

For Na-TNW, acetonitrile desorbs at temperature of 50-520°C (6.31 mmol). The amount of acetonitrile is less than that on two titanate nanotubes and commercial P25 TiO_2. This is because the Na-TNW is not hollow structure but it is dense, as seen by the lower surface area (Table 4.1). The desorption temperature of acetonitrile on Na-TNW is less than that for the other three materials, suggesting that the interaction between acetonitrile and Na-TNW are weaker than that with other nanostructure adsorbents.

The larger amount of desorbed acetonitrile in these titanate nanotubes could be due to their relatively high surface area, as reported by several authors [47]. Titanate nanotubes are long and hollow objects. This nanostructure might allow the interaction with acetonitrile molecules both at the internal and the external surfaces. In particular, nanotube ion exchanged with $BaCl_2$ desorbed acetonitrile molecules at higher temperature (457 °C) than Na-TNT (283 °C) and commercial P25 TiO_2 (360 °C). These results might be explained considering that Ba^{2+} has higher charge than Na^+. The interactions of Ba^{2+} with acetonitrile should be stronger than those of Na^+.

Commercial P25 TiO_2 desorbed acetonitrile in the range 50-500°C as shown in **Figure 4.10(d)**. The desorbed amount is 6.54 mmol/g. This value is smaller than the amount desorbed from Na-TNT shown in **Figure 4.10(b)** (9.45 mmol/g, 50-360°C), and from Ba-TNT as shown in **Figure 4.10(c)** (15.22 mmol/g, 50-645°C).

The first component (component i) appears at 130-143° C. This desorption peak can be explained by the physisorption on the surface. The desorption temperature is higher than that of acetone (118-137 °C), indicating the strong interaction of materials with acetonitrile. The second component (component ii) shows the peak at temperature around 210-244 °C (vs 167-217 °C for acetone). This can be explained by the chemisorption of acetonitrile, as shown in **Scheme 4.3.**

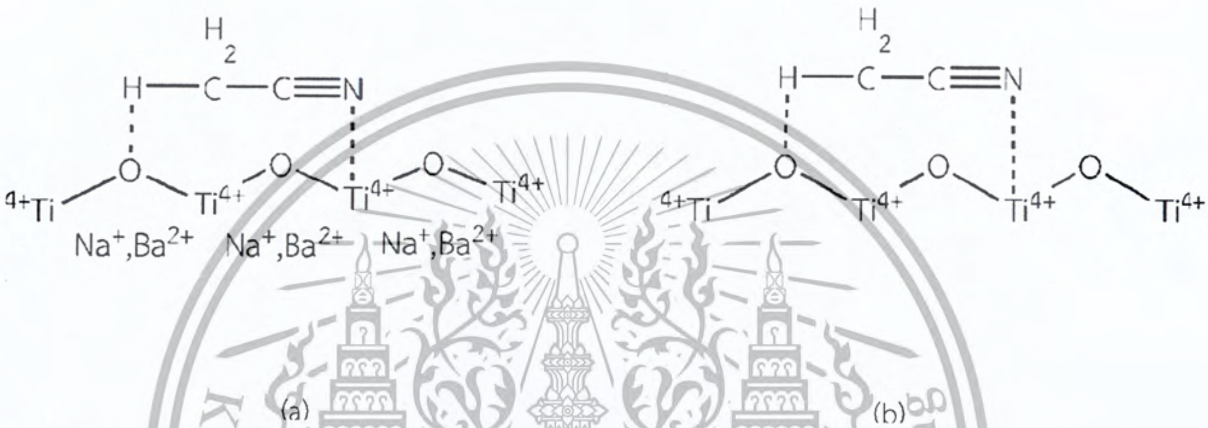

Scheme 4.3 Schematic illustration of the chemisorption showing the interactions of an acetonitrile molecule with the surfaces of (a) Na-TNW and Na- and Ba-TNT, (b) commercial P25 TiO_2.

The last component (component iii) appears in the range 283-457 °C (vs 255-367 °C for acetone). Unlike acetone, this component (component iii) cannot be described as the condensation of acetonitrile. Hence, it is suggested that it is due to the desorption of water molecules contained in acetonitrile. The water molecule could interact with Ti^{4+} via hydroxylation reaction upon the adsorption. This hydroxylated titanate can be decomposed at high temperature, as demonstrated by **Scheme 4.4**.

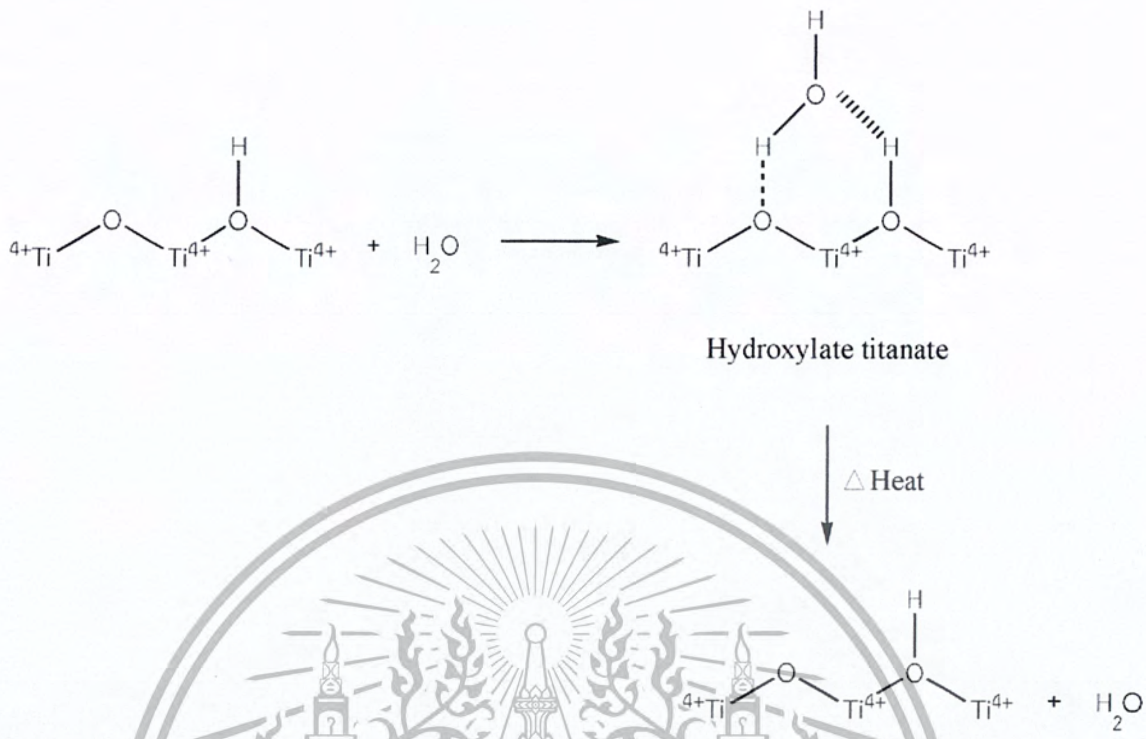

Scheme 4.4 The dehydroxylation on the surfaces of nanotubes resulting in the desorption of water

On Na-TNW and commercial P25 TiO_2, the larger fraction of desorbed acetonitrile is at low temperature. This suggests that the majority of surfaces species on Na-TNW and commercial P25 TiO_2 is the physisorbed acetonitrile. On Na-TNT and Ba-TNT, however, the majority of the desorbed species is the chemisorbed acetonitrile. In addition, the desorption of water contaminating acetonitrile can be largely observed, as compared to Na-TNW and commercial P25 TiO_2. This suggests that Na- and Ba-TNT interact with water stronger than Na-TNW and commercial P25 TiO_2.

Comparing the desorption temperature of acetone and acetonitrile, it was found that the desorption temperature of acetonitrile are higher than that of acetone on the titanate-based adsorbents (Na-TNW, Na-TNT, Ba-TNT, and commercial P25 TiO_2). This is because the CN group of acetonitrile is highly polar, as compared to the carbonyl group of acetone. Accordingly, the interaction between acetonitrile and the adsorbents could be stronger than that for acetone.

CHAPTER 5

CONCLUSIONS AND SUGGESTIONS

5.1 Conclusion

Lepidocrocite titanate with the composition of KZn was successfully prepared by solid state synthesis. Potassium ions in $K_{0.8}Zn_{0.4}Ti_{1.6}O_4$ were replaced with protons of HCl by proton exchange process. However, not only proton has been exchanged. The framework Zn was also leached. The structural composition of the product after proton exchange will be then referred to as "$H_{1.6}\square_{0.4}Ti_{1.6}O_4 \cdot 0.8H_2O$". The identity of this product was confirmed by PXRD and TGA. The protonated lepidocrocite titanate ($H_{1.6}\square_{0.4}Ti_{1.6}O_4 \cdot 0.8H_2O$) was exfoliated with tetrabutylammonium hydroxide (TBAOH). After the exfoliation, the colloidal suspension obtained indicates the separation of stacks of titanate layers into individual ones. The colloids show the characteristics light adsorption at 262 nm. After that, the colloidal suspension was reassembled by KCl (and $BaCl_2$). The reassembled titanate nanosheets were then obtained.

The $Na_2Ti_3O_7$ was prepared by solid state synthesis. Sodium ions in $Na_2Ti_3O_7$ were replaced with protons of HCl via proton exchange process. The product from the proton exchange of $Na_2Ti_3O_7$ will be here after called "$H_2Ti_3O_7$". $H_2Ti_3O_7$ was exfoliated with tetrametylammonium hydroxide (TMAOH). After the exfoliation the mixture did not change into colloid. The Tyndall effect could not be observed. Similarly, reaction under a hydrothermal condition did not give the colloid. One can conclude that the attraction between sheets of $H_2Ti_3O_7$ is so strong that TMA^+ cannot penetrate into the layers. Hence, the exfoliation of $H_2Ti_3O_7$ by TMA^+ was not possible.

Na-TNW was successfully prepared from P25 and 10M NaOH by a hydrothermal method.

The titanate-based materials were studied as sorbents for acetone and acetonitrile. Materials tested included lepidocrocite titanate KZn, K-rKZn and Ba-rKZn, Na-TNW, Na-TNT, Ba-TNT and commercial P25 TiO_2. The results show that lepidocrocite titanate KZn and K-rKZn and Ba-rKZn cannot adsorb acetone and acetonitrile. Moreover, these structures might collapse when heated at high temperature (up to 800 °C). However, Na-TNW can adsorb both acetone and acetonitrile, but with a less extent, as compared to Na-TNT, Ba-TNT and commercial P25 TiO_2. This is because the structure of Na-TNW is dense with low surface area. In addition, Na-TNW gives no condensation product from acetone. On the other hands, Na-TNT, Ba-TNT and commercial P25 TiO_2 give condensation products from acetone. This result might be because the Na-TNW retains the rutile structure that contains less number of defects. A higher amount of acetone and acetonitrile can be adsorbed Ba-TNT, as compared to other titanate nanomaterials. The result may be explained considering that the nanotube has high surface area. However, Ba-TNT gives higher products from the condensation of acetone, as compared to Na-TNT. This is because the interactions of Ba^{2+} with acetone (acetonitrile) are stronger than those of Na^{+}.

The desorption temperatures of acetonitrile are higher than those of acetone on the titanate-based adsorbents. This is because the CN group in acetonitrile is more polar than the carbonyl group of acetone. Hence, the interactions between acetonitrile and the nanomaterial absorbents are stronger than those with acetone.

5.2 Suggestions

The Ba-TNT can adsorb a large concentration of acetone and acetonitrile. Hence, it will be interesting to study about the effect of other cations in addition to Na^{+} and Ba^{2+} in the adsorption of VOCs.

REFERENCE

[1] **"Titanium dioxide."** [Online]. Available :
https://en.wikipedia.org/wiki/Titanium_dioxide

[2] P. Kaewmora, W. Maneerattanaamorn, W. Netrungruang. 2015. **"Preparation of self-cleaning glass by coating with lepidocrocite titanate nanosheets." Faculty of science, KMITL 1.**

[3] K. Limsakul, S. Juntarachairot, S. Sangsan. 2013. **"Deoxygenation of palmitic acid with catalyst based on lepidocrocite titanates." Faculty of science, KMITL 1.**

[4] **"ความรู้เบื้องต้นเกี่ยวกับสารอินทรีย์ระเหยง่าย (VOCs)."** [Online]. Available :
http://www.industry.in.th/dip/knowledge_detail.php?id=1165&uid=35317

[5] TV. Dinh, IY. Choi, YS. Son, KY. Song, Y. Sunwoo, JC. Kim. 2016. **"Volatile organic compounds (VOCs) in surface coating materials: Their compositions and potential as an alternative fuel."** Journal of Environmental Management. 168 : 157-164.

[6] **"Volatile Organic Compounds."** [Online]. Available :
http://www.en.mahidol.ac.th/elearning/upload/Org_2013_Lec3.pdf

[7] Y. Dumanoglu, M. Kara, H. Altiok, M. Odabasi, T. Elbir, A. Bayram. 2014. **"Spatial and seasonal variation and source apportionment of volatile organic compounds (VOCs) in a heavily industrialized region." Atmospheric Environment. 98 : 168-178.**

[8] G. Gałezowska, M. Chraniuk, L. Wolska. 2016. **"In vitro assays as a tool for determination of VOCs toxic effect on respiratory system: A critical review."** Trends in Analytical Chemistry. 77 : 14-22.

[9] **"Volatile organic compounds (Acetone)."** [Online]. Available :
https://en.wikipedia.org/wiki/Acetone

[10] **"Acetone."** [Online]. Available : http://goo.gl/aUKzWP

[11] DG. Lee, JH. Kim, CH. Lee. 2011. **"Adsorption and thermal regeneration of acetone and toluene vapors in dealuminated Y-zeolite bed."** Separation and Purification Technology. 77 : 312-324

[12] **"MSDS of acetone."** [Online]. Available :
http://physics.utsa.edu/memslab/MSDS/Acetone.pdf

[13] **"Acetone structure."** [Online]. Available : https://goo.gl/tyqh7C

[14] **"Acetonitrile."** [Online]. Available : https://en.wikipedia.org/wiki/Acetonitrile

[15] **"Acetonitrile msds."** [Online]. Available :
http://www.sciencelab.com/msds.php?msdsId=9927335

[16] **"Titanium dioxide:TiO_2."** [Online]. Available : http://goo.gl/2ns3Ao

[17] **"TiO_2 structure."** [Online]. Available : https://goo.gl/LcEGWu

[18] S. Ribbens, V. Meynen, G. Van Tendeloo, X. Ke, M. Mertens,
B. Maes , P. Cool, E.F. Vansant. 2008. **"Development of photocatalytic efficient Ti-based nanotubes and nanoribbons by conventional and microwave assisted synthesis strategies."** Microporous and Mesoporous Materials. 114 : 401-409.

[19] O. V. Yakubovich, V. V. Kireev. 2003. **"Refinement of the crystal Structure of $Na_2Ti_3O_7$."** Crystallography Reports. 48 : 24-28.

[20] T. Gao, H. Fjellvag, P. Norby. 2009. **"Raman scattering properties of a protonic titanate $H_xTi_{2-x/4}0_{x/4}O_4 \cdot H_2O$ (□, vacancy; x = 0.7) with lepidocrocite-type layered structure."** Journal Physical Chemistry. 31 : 9400-9405.

[21] T. Gao, H. Fjellvag, P. Norby. 2009. **"Defect chemistry of a zinc-doped lepidocrocite titanate $C_{sx}Ti_{2-x/2}Zn_{x/2}O_4$ (x=0.7) and its protonic form."** Chemistry of materials. 21 : 3503-3513.

[22] **"Nanomaterial."** [Online]. Available :
http://eng.thesaurus.rusnano.com/upload/iblock/dfc/nanomaterial1.jpg

[23] M.N. Asiah, M.H.Mamat, Z.Khusaimi, S.Abdullah, M.Rusop, A. Qurashi. 2015. **"Surfactant-free seed-mediated large-scale synthesis of mesoporous TiO_2 nanowires."** Ceramics International. 41 : 4260-4266.

[24] L. Li, X. Qin, G. Wang, L. Qi, G. Du, Z. Hu. 2011. **"Synthesis of anatase TiO_2 nanowires by modifying TiO_2 nanoparticles using the microwave heating method."** Applied Surface Science. 257 : 8006-8012.

[25] J. Jitputti, Y. Suzuki, S. Yoshikawa. 2008. **"Synthesis of TiO_2 nanowires and their photocatalytic activity for hydrogen evolution."** Catalysis Communications. 9 : 1265-1271.

[26] CL. Wong, YN. Tan, AR. Mohamed. 2011. **"A review on the formation of titania nanotube photocatalysts by hydrothermal Treatment."** Journal of Environmental Management. 92 : 1669-1680.

[27] **"Titanate nanotubes."** [Online]. Available :
http://link.springer.com/article/10.1007%2Fs10853-007-2374-3

[28] **"Nanosheets."** [Online]. Available : https://en.wikipedia.org/wiki/Nanosheet

[29] **"Two-Dimensional nanosheets."** [Online]. Available :
http://onlinelibrary.wiley.com/doi/10.1002/adma.201103241/abstract

[30] **"2D layered titanate nanosheets."** [Online]. Available :
http://digital.csic.es/bitstream/10261/95421/4/Artificially%20Stacked%20Atomic.pdf

[31] **"Surface of titanium dioxide."** [Online]. Available :
http://spie.org/newsroom/3894-enhanced-solar-water-splitting-by-surface-engineering-of-titanium-dioxide

[32] J. Feng, L. Zou, Y. Wang, B. Li, X. He, Z. Fan, Y. Ren, Y. Lv, M. Zhang, D. Chen. 2015. **"Synthesis of high surface area, mesoporous MgO nanosheets with excellent adsorption capability for Ni(II) via a distillation treating."** Journal of Colloid and Interface Science. 438 : 259-267.

[33] A. Jain, R. Balasubramanian, M.P. Srinivasan. 2015. **"Production of high surface area mesoporous activated carbons from waste biomass using hydrogen peroxide-mediated hydrothermal treatment for adsorption applications."** Chemical Engineering Journal. 273 : 622-629

[34] AH. Bergerand, AS. Bhown. 2011. **"Comparing Physisorption and Chemisorption Solid Sorbents for use Separating CO_2 from Flue Gas using Temperature Swing Adsorption."** Energy Procedia. 4 : 562-567.

[35] **"Adsorption Desorption."** [Online]. Available :
http://www.chromatographytoday.com/news/hplc-uhplc/31/breaking_news/adsorption_absorption_and_desorption_whats_the_difference/31397/

[36] **"Desorption."** [Online]. Available : https://en.wikipedia.org/wiki/Desorption

[37] **"Desorption process."** [Online]. Available :
http://www.chem.qmul.ac.uk/surfaces/scc/scat2_6.htm

[38] CK. Lee, HC. Chen, SS. Liu, FC Huang. 2010. **"Effects of acid washing treatment on the adsorption equilibrium of volatile organic compounds on titanate nanotubes."** Journal of the Taiwan Institute of Chemical Engineers. 41 : 373-380.

[39] A. Maudhuita, C. Raillard, V. Héquet, LL. Coqa, J. Sablayrolles, L. Molins. 2011. **"Adsorption phenomena in photocatalytic reactions: The case of toluene, acetone and heptane."** Chemical Engineering Journal. 170 : 464-470.

[40] I. Ushiki, M. Ota, Y. Sato, H Inomata. **2015. "VOCs (acetone, toluene, and n-**

hexane) adsorption equilibria on mesoporous silica (MCM-41) over a wide range of supercritical carbon dioxide conditions: Experimental and theoretical approach by the Dubinin–Astakhov equation." Fluid Phase Equilibria. 403 : 78-84.

[41] F. Qu, L. Zhu, K. Yang. 2009. "Adsorption behaviors of volatile organic compounds (VOCs) on porous clay hetero structures (PCH)." Journal of Hazardous Materials. 170 : 7-12.

[42] N. Takahashi, I. Ushiki, Y. Hamabe, M. Ota, Y. Sato, H. Inomata. 2016. "Measurement and prediction of desorption behavior of five volatile organic compounds (acetone, n-hexane, methanol, toluene, and n-decane) from activated carbon for supercritical carbon dioxide regeneration." Journal of Supercritical Fluids. 107 : 226-233.

[43] S. Zuo, F. Liu, R. Zhou, C. Qi. 2012. "Adsorption/desorption and catalytic oxidation of VOCs on montmorillonite and pillared clays." Catalysis Communications. 22 : 1-5.

[44] J. Xu, B. Mojet, J. Ommen, L. Lefferts. 2004. "Desorption of Acetone from Alkaline-Earth Exchanged Y Zeolite after Propane Selective Oxidation." Jounal of Physics and Chemistry. 108 : 218-223.

[45] B. Lin, Y. Zhou, L. He, W. Yang, Y. Chen, B. Gao. 2015. "Mesoporous CdS-pillared $H_2Ti_3O_7$ nanohybrids with efficient photo-catalytic activity." Journal of Physics and Chemistry of Solids. 79 : 66-71.

[46] D. Groult, C. Mercey, B. Raveau. May,1980. "Nouveaux oxydes à structure en feuillets: Les titanates de potassium non-stoechiométriques $K_x(M_yTi_{2-y})O_4$." Journal of Solid State Chemistry. 32(3) : 289–296.

[47] L. Zhenhua, L. Zhongqing, Y. Qingzhi, W. Yichao, G. Changchun. 2008. "Preparation and performance of titanate nanotube by hydrothermal treatment." RARE METALS., Vol. 27, 2008. pp.187.

APPENDICES

APPENDIX A

CALCULATION

Calculation of the solid state synthesis of lepidocrocite titanate (30g)

$$0.4K_2CO_3 + 1.6TiO_2 + 0.4ZnO \longrightarrow K_{0.8}Zn_{0.4}Ti_{1.6}O_4 + 0.4CO_2$$

Weight of K_2CO_3;

$$\frac{\text{mol } K_2CO_3}{\text{mol } K_{0.8}Zn_{0.4}Ti_{1.6}O_4} = \frac{0.4}{1}$$

$$\frac{\frac{g\ K_2CO_3}{MW\ K_2CO_3}}{\frac{g\ K_{0.8}Zn_{0.4}Ti_{1.6}O_4}{MW\ K_{0.8}Zn_{0.4}Ti_{1.6}O_4}} = \frac{0.4}{1}$$

$$g\ K_2CO_3 = \frac{0.4}{1} \times \frac{g\ K_{0.8}Zn_{0.4}Ti_{1.6}O_4}{MW\ K_{0.8}Zn_{0.4}Ti_{1.6}O_4} \times MW\ K_2CO_3$$

$$g\ K_2CO_3 = \frac{0.4}{1} \times \frac{30\ g}{197.84} \times 138.205$$

$$g\ K_2CO_3 = 8.3719\ g$$

Weight of TiO_2;

$$\frac{\text{mol } TiO_2}{\text{mol } K_{0.8}Zn_{0.4}Ti_{1.6}O_4} = \frac{1.6}{1}$$

$$\frac{\frac{g\ TiO_2}{MW\ TiO_2}}{\frac{g\ K_{0.8}Zn_{0.4}Ti_{1.6}O_4}{MW\ K_{0.8}Zn_{0.4}Ti_{1.6}O_4}} = \frac{1.6}{1}$$

$$g\ TiO_2 = \frac{1.6}{1} \times \frac{g\ K_{0.8}Zn_{0.4}Ti_{1.6}O_4}{MW\ K_{0.8}Zn_{0.4}Ti_{1.6}O_4} \times MW\ TiO_2$$

$$g\ TiO_2 = \frac{1.6}{1} \times \frac{30\ g}{197.84} \times 79.866$$

$$g\ TiO_2 = 19.3771\ g$$

Weight of ZnO; $$\frac{\text{mol ZnO}}{\text{mol } K_{0.8}Zn_{0.4}Ti_{1.6}O_4} = \frac{0.4}{1}$$

$$\frac{\frac{\text{g ZnO}}{\text{MW ZnO}}}{\frac{\text{g } K_{0.8}Zn_{0.4}Ti_{1.6}O_4}{\text{MW } K_{0.8}Zn_{0.4}Ti_{1.6}O_4}} = \frac{0.4}{1}$$

$$\text{g ZnO} = \frac{0.4}{1} \times \frac{\text{g } K_{0.8}Zn_{0.4}Ti_{1.6}O_4}{\text{MW } K_{0.8}Zn_{0.4}Ti_{1.6}O_4} \times \text{MW ZnO}$$

$$\text{g ZnO} = \frac{0.4}{1} \times \frac{30 \text{ g}}{197.84} \times 81.40$$

$$\text{g ZnO} = 4.9378 \text{ g}$$

The calculation of mmol of acetone and acetonitrile from the TCD

- The injection of 0.1 μL (at atmospheric pressure) of acetone gives rise to the peak area of 0.4119 unit. The temperature of the TCD is set at 50 °C.

Density acetone at 50 °C = 757.332 kg/m^3 = 757.332×10^{-3} kg/L

$$D = \frac{m}{V} \longrightarrow m = DV = (757.332\times10^{-3}\ \text{kg/L})(0.1\times10^{-6}\ \text{L})$$

$$m = 7.5733\times10^{-8}\ \text{kg}$$

The molecular mass of acetone is 58.08 g/mol, or 58.08×10^{-3} kg/mol

$$\text{mol} = \frac{\text{g}}{\text{Mass molecule}} = \frac{7.5733\times10^{-8}\text{kg}}{58.08\times10^{-3}\text{kg/mol}} = 0.0013\ \text{mmol}$$

So, peak area 0.4119 equals acetone 0.0013 mmol. This relationship was used for the conversion of peaks area of desorbed actone to mmol of acetone.

- The injection of 0.1 μL of acetonitrile gives the signal by TCD with the peak area 0.6209 unit.

Density acetonitrile at 50 °C = 750.982 kg/m^3 = 750.982×10^{-3} kg/L

$$D = \frac{m}{V} \longrightarrow m = DV = (750.982\times10^{-3}\ \text{kg/L})(0.1\times10^{-6}\ \text{L})$$

$$m = 7.5098\times10^{-8}\ \text{kg}$$

The molecular mass of acetonitrile is 41.05 g/mol, or 41.05×10^{-3} kg/mol.

$$\text{mol} = \frac{\text{g}}{\text{Mass molecule}} = \frac{7.5098\times10^{-8}\text{kg}}{41.05\times10^{-3}\text{kg/mol}} = 0.0018 \text{ mmol}$$

So, peak area 0.6209 equals the amount of acetonitrile of 0.0018 mmol

APPENDIX B

ADSORPTION DATA

Table B1: Summary of the deconvolution of the acetone-TPD profiles of lepidocrocite titanate KZn, K-rKZn and Ba-rKZn. As discussed in the main text, these desorption peaks are considered as the decomposition products of the materials but not the desorption of acetone.

Adsorbent	Total area/g	Total mmol/g	Component i				Component ii			
			$T_{initial}$	T_{peak}	T_{fiant}	mmol/g	$T_{initial}$	T_{peak}	T_{final}	mmol/g
Lepidocrocite titanate KZn	103.45	0.0	445°C	603°C	790°C	0.0	650°C	720°C	800°C	0.0
K-rKZn	3069.68	0.9	553°C	720°C	880°C	0.6	714°C	802°C	880°C	0.3
Ba-rKZn	3434.64	1.1	534°C	723°C	900°C	0.9	750°C	821°C	900°C	0.2